AALBORG UNIVERSITY
DENMARK

Parameterization of Respiratory Peripheral Drive in Spontaneously Breathing Patients with Central Drive Depression

Esben Bolvig Mark & Kasper Sørensen
Department of Health Science and Technology
Aalborg University

Master's Thesis
Spring 2015

AALBORG UNIVERSITET

Department of Health Science and Technology

hst.aau.dk

Title:

Parameterization of Respiratory Peripheral Drive in Spontaneously Breathing Patients with Central Drive Depression

Subject:

Applied biomedical engineering and informatics

Project period:

Spring 2015

Project group:

15GR1076

Authors:

Esben Bolvig Mark
M.Sc. Student

Kasper Sørensen
M.Sc. Student

Supervisors:

Lars Pilegaard Thomsen
Assistant Professor, PhD., M.Sc.
Aalborg University

Stephen Edward Rees
Professor
Aalborg University

Abstract

The respiratory drive of the individual patient is of clinical interest to the clinician as this parameter might contribute to an improved treatment. The physiological theories of the mechanisms of respiratory drive is well described. The respiratory control consists mainly of two chemoreflexes that respond to arterial carbon dioxide and oxygen pressure referred to as the central and the peripheral drive control respectively.

Measuring the respiratory drive and determining the contributions of the different drives is not a trivial task. In order to do so a set of mathematical models can be used. Using a sample of arterial blood gas and clinically available parameters for pulmonary gas exchange obtained with the bedside tool ALPE, the respiratory drive of the patient can be parameterized and changes in the patient's respiration due to change in ventilator settings can be estimated.

The current version of the model of respiratory drive parameterizes the central drive threshold of the patient. The model have not previously been tested on patients with spontaneous breathing and with no mechanical ventilation.

This thesis introduces a novel method for parameterization and estimation of the peripheral drive of spontaneously breathing patients. The patients included in the selected test group are diagnosed with COPD. This patient group is known to have a reduced central drive. Reduction in central drive poses a threat to the patient, because an increased arterial oxygen pressure may then cause hypoventilation and hypoxemia. Patients submitted to oxygen treatment as in the post-operative period may experience increased arterial oxygen pressure.

Four simple parameter estimation methods are tested in order to estimate the peripheral drive in six spontaneously breathing patients. The methods includes a parameter estimation of different peripheral drive parameters using a grid search algorithm. The four methods of parameter estimation are evaluated both by visually inspection and calculation of mean squared error between measured and estimated alveolar ventilation.

Parameterization of the peripheral drive may be used to describe and predict respiratory response to changes in oxygen treatment at the bedside.

Resumé

Viden om en patients respiratoriske drive kan bidrage til en forbedret behandling. De fysiologiske teorier bag respirationskontrol beskriver, at respirationen hovedsageligt er styret af to kemoreflekser, der reagerer på ændringer i arterielle tryk af kuldioxid og oxygen. Den kuldioxidfølsomme refleks kaldes det centrale drive og den oxygenfølsomme refleks kaldes det perifere drive.

Det er ikke trivielt at bestemme de to drives bidrag til den samlede ventilation, da de ikke kan måles direkte. Der er udviklet et sæt af matematiske modeller, der kan estimere ventilationsbidragene ud fra en arteriel blodgas-prøve og parametre for respiratorisk gasudveksling der er tilgængelig fra det kliniske måleudstyr ALPE. Det respiratoriske drive kan herved parametriseres for en patient, hvilket kan hjælpe til at give beslutningsstøtte i forhold til ændring af respiratorindstillinger.

Den nuværende version af modellen kan parametrisere en patients centrale drive, men er ikke tidligere blevet testet på patienter med spontan vejrtrækning, der ikke er i respiratorbehandling.

Denne specialeopgave introducerer en metode til parametrisering og estimering af perifert drive for patienter med spontan vejrtrækning. Den inkluderede patientgruppe består af patienter diagnosticeret med KOL. Denne patientgruppe er blandt andet karakteriseret ved nedsat centrale drive. Nedsat centralt drive kan være farligt, hvis patienten er under oxygenbehandling, da øget arterielt ilttryk kan medføre hypo-ventilation og hypoxæmi grundet.

Fire simple parameterestimeringsmetoder er blevet testet for at estimere det perifere drive i seks KOL-patienter med spontan vejrtrækning. Metoderne estimerer forskellige perifere drive-parametre, som kan beskrive hvordan ændringer i inspiratoriske iltfraktioner kan påvirke ventilationen. Metoderne er baseret på en grid-search algoritme. De tre metoder er vurderet ud fra visuel inspektion af resultater samt udregning af mean squared error imellem de målte og estimerede værdier for alveolær ventilation.

Parametrisering af det perifere drive kan være brugbart til at beskrive og forudsige respiratorisk respons til ændringer i oxygen behandling.

Preface

This project is written by Esben Bolvig Mark and Kasper Sørensen as the master's thesis in the M.Sc. in Biomedical Engineering and Informatics at Aalborg University, spring 2015.

The thesis is divided into four main parts: Background, Method, Results and Synthesis. A basic understanding of the human respiratory physiology is required by the reader to fully understand the content of this thesis.

Literature in the project are stated using the Harvard-method, with the following syntax: [Author's last name, Publication year]. The reader can find more information about the references in the literature list, where the references are listed in alphabetic order according to the author's last name.

References to figures, tables, chapters and so forth are stated according to what object is referred to and in what section it is placed. The first figure placed in chapter two will therefore be referred to as Figure 2.1. The next will be Figure 2.2 and so forth.

Esben Bolvig Mark Kasper Sørensen

Spring - 2015 - Aalborg University

Contents

IV Synthesis

PART I

BACKGROUND

CHAPTER 1

Introduction

The respiratory drive of the individual patient, and especially those in need of mechanical ventilation, is a subject of interest for researchers [Duffin, 2005; Larraza et al., 2014]. Estimation of individual respiratory drive will allow clinical staff to optimize patient treatment [Larraza et al., 2014]. The theories of the respiratory control centers are well established, thus there exists an understanding of how respiratory ventilation is affected by changes in arterial oxygen (P_aO_2) and arterial carbon dioxide (P_aCO_2) [Duffin, 2005; Lumb, 2010]. These theories are based on the effects of the central and peripheral chemoreceptors on the respiratory ventilation.

Measurement of respiratory drive in the individual patient is not a trivial task. A set of mathematical models with the purpose of estimating the underlying chemical components of the respiratory drive, pulmonary gas exchange, blood acid-base status and lung mechanics have been developed [Duffin, 2005; Larraza et al., 2014; Rees & Andreasen, 2005; Rees et al., 2002]. These models parameterize, among others, the chemical components for the individual patient and can thereby be used to estimate the individual respiratory drive. The models have been clinically tested on 12 mechanical ventilated, spontaneously breathing patients. The models have been evaluated and adequately describes data for the patients for who the models were tested [Larraza et al., 2015a,b].

The models have not been tested on spontaneous breathing patients, who are not mechanical ventilated. A patient group of interest is patients in the post-operative period. In the post-operative period where the effect of anesthesia is still wearing off, pulmonary oxygenation might be impaired [Hedenstierna, 2012]. In the post-operative period, modulations of the respiratory drive is thought of to be difficult to predict, but is of great value for the clinicians.

The knowledge of individual patient respiratory drive response might help to predict unwanted complications of post-operative apnoea or hypoxia [Lumb, 2010].

1.1 Project Aim

Establish whether and how a modeling approach may be used to estimate respiratory peripheral drive in spontaneously breathing patients.

1.2 Solution Strategy

The approach to solve the project aim is divided into three main parts.

Part I: Background
The first part of this project consists of an introduction to the physiology of the respiratory chemoreceptor control. This part aims to describe the two main components of the respiratory drive, namely the central and peripheral drive. Furthermore the physiologic section will explain how the respiratory drive response is impaired in some patients in the post-operative period. This will provide an understanding of why it is of clinical value to estimate a patient's respiratory response.

Part II: Methods
The next part of this project aims to explain one of the current models for estimating respiratory drive. Understanding the respiratory model will allow for identification of the limitations associated with using the model.
This part will furthermore examine the model's estimation of peripheral drive response in order to evaluate whether or not the model can be used to adequately describe patients' respiratory drive in a patient group, that has not previously been examined with the model. As the model's central respiratory response estimation has previously been evaluated by Larraza et al., 2015a,b, this project will focus on the peripheral drive response and hence the response to changes in oxygen (hypoxia).
The chapter "Peripheral Drive Modeling" will describe the steps that were carried out in order to develop a method for parameterization of the peripheral drive.
A novel method for estimating peripheral drive will be proposed. This method aims to parameterize the peripheral drive to give a patient specific estimation of the patients response to changes in oxygen.

Part III: Results
The methods for estimation of peripheral drive will be evaluated using patient data obtained from a clinical trial. These patients are diagnosed with COPD and are thereby members of a patient group known to have an impaired central drive [Larraza et al., 2015b; Lumb, 2010].

CHAPTER 2

Physiology

2.1 Chemical Control of Respiration

The pressure of carbon dioxide in the blood ($PaCO_2$) is controlled by the respiratory chemoreflexes to ensure that the hydrogen ion concentration $[H^+]$ is within the constrained limits for protein function [Duffin, 2005].

The respiratory chemoreflexes are produced by two types of chemoreceptors, central and peripheral, which are named accordingly to their location compared to the respiratory center in the medulla [Hall, 2010]. The functions of the two chemoreceptors will be described in the following sections.

2.1.1 Central Chemoreceptors

The respiratory center located in the medulla oblangata is not by itself affected directly by changes in blood concentrations of P_{CO_2} and $[H^+]$ [Hall, 2010]. A chemosensitive area located 0.2 millimeter beneath the surface in the medulla is highly sensible to changes in arterial P_{CO_2} or $[H^+]$ ion concentrations in the blood. This area is referred to as the central chemoreceptors and its primary function is to excite other areas in the respiratory center to control the respiration pattern [Hall, 2010].

The chemosensitive area in the medulla is almost only excited by hydrogen ions, but hydrogen ions in the blood can not directly cross the blood-brain barrier. The medulla oblangata is like the rest of the brain protected by the blood-brain barrier, which is impairing the diffusion of charged ions from arterial blood to cerebrospinal fluid (CSF) [Hall, 2010]. Change in blood P_{CO_2} is much more effective in comparison to change in hydrogen ion concentration in reaching the chemosensitive area and hereby influence the respiration. Carbon dioxide has little direct effect in stimulating the chemosensitive area, but by reacting with water from the tissue, the carbon dioxide is transformed into carbonic acid and further into hydrogen and bicarbonate ions, which have a direct stimulating effect on the respiration [Hall, 2010]. Hereby the central chemoreceptors are contributing to the respiratory drive by adding a hypercarbic sensitive drive, which furthermore is the most contributing drive to breath in a healthy person.

2.1.1.1 Carbon Dioxide / Ventilation Response Curve

The P_{CO_2}/ventilation response curve describes how changes to the arterial P_{CO_2} affect the respiratory minute volume see Figure 2.1 [Lumb, 2010]. This linear response is manifested as an increased minute volume, if arterial P_{CO_2} is raised. The raised ventilation ensures that excess CO_2 is expelled from the blood, thereby lowering the alveolar P_{CO_2} to a normal level.

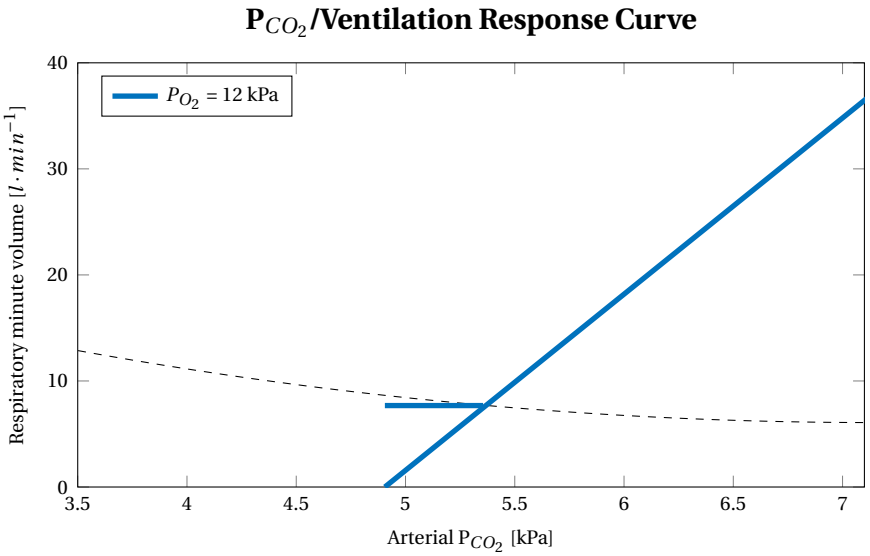

Figure 2.1: *Stylistic P_{CO_2}/ventilation response curve. In this example arterial P_{O_2} is assumed to be a normal 12 kPa. Two cases of respiratory response to change in P_{CO_2} are presented, see further explanation in the text. Drawn with inspiration from [Lumb, 2010].*

A typical normal P_{CO_2}/ventilation response curve has a slope of 15 l·min^{-1}·kPa^{-1} as shown in Figure 2.1. The intercept at zero ventilation is 4.8 kPa for a typical normal case [Lumb, 2010]. The slope and the intercept at zero ventilation defines the linear relationship between ventilation and arterial P_{CO_2} and can be described by Equation 2.1a with S being the slope and B the intercept at zero ventilation. For a normal situation this would yield a curve described by Equation 2.1b. It should be noted that this normal curve is subject to a wide variation among individuals [Lumb, 2010].

$$\text{ventilation} = S \cdot (P_{CO_2} - B) \tag{2.1a}$$

$$\text{ventilation} = 15 \frac{l}{min \cdot kPa} \cdot (P_{CO_2} - 4.8kPa) \tag{2.1b}$$

In Figure 2.1 the intersection between the broken curve and the P_{CO_2}/ventilation response curve indicates normal P_{CO_2} and ventilation. The broken line represents ventilation at zero inspired P_{CO_2} for

normal metabolic rate [Lumb, 2010]. The broken line thereby represents changes to arterial P_{CO_2} caused by changing ventilation at normal inspired CO_2 (≈ 0 kPa).

Figure 2.1 shows two possible cases of change in ventilation based on P_aCO_2 below the broken line for the normal situation. In the first case, ventilation decreases linearly with respect to P_aCO_2. The intersection between the P_aCO_2 curve and the X-axis is known as the apnoeic threshold [Lumb, 2010]. If P_aCO_2 is decreased below this threshold apnoea may occur for some patients.

In the second case, drawn as a "hockey stick" see Figure 2.1, the ventilation does not decrease regardless of the decrease in arterial P_{CO_2}. This is most commonly the case in humans [Lumb, 2010].

2.1.2 Peripheral Chemoreceptors

The peripheral chemoreceptors are unlike the central chemoreceptors located outside the brain and the respiratory center. These chemoreceptors are located in the carotid bodies and the aortic bodies, with the majority of receptors in the carotid bodies, why they are at all time exposed to arterial blood. The peripheral chemoreceptors are important in detecting change in blood oxygen pressure [Hall, 2010].

The chemoreceptors are stimulated when the arterial P_{O_2} is decreasing [Lumb, 2010], why the peripheral chemoreceptors are sensitive to hypoxemia. The excitation rate of the receptors are peaking in the range of arterial P_{O_2} from 4 to 8 kPa (normal values of arterial P_{O_2} are 10-13.3 kPa) [Hall, 2010].

Change in P_aCO_2 and $[H^+]$ likewise have an effect on the peripheral chemoreceptors [Hall, 2010]. The effect is though approximately seven times higher in the central chemoreceptors compared to the peripheral, why it for practical reasons often can be ignored. The peripheral chemoreceptors are reacting five times more rapidly to stimulation than the central receptors, thus the stimulation can be important in exercise despite the lower response to changes in blood concentration [Hall, 2010].

2.1.2.1 Oxygen / Ventilation Response Curve

Just as with the respiratory response to changes in arterial P_{CO_2} the respiratory response to changes in arterial P_{O_2} can be visualized. In Figure 2.2 a stylistic example shows how changes to arterial P_{O_2} affects the respiratory ventilation [Lumb, 2010]. The blue line in Figure 2.2 resembles normal arterial P_{O_2}. The green and red line illustrates high and low arterial P_{O_2} respectively. In Figure 2.2 it is seen that a 6.6 fold increase in arterial P_{O_2} only has little effect on the respiratory response to changes in arterial P_{CO_2} compared to the respiratory response of a relatively low decrease in arterial P_{O_2}. Hence lower-

ing inspired O_2 and thereby lowering arterial P_{O_2} will cause rapid increase in respiratory ventilation as response to a rise in arterial P_{CO_2}, compared to a normal situation [Lumb, 2010].

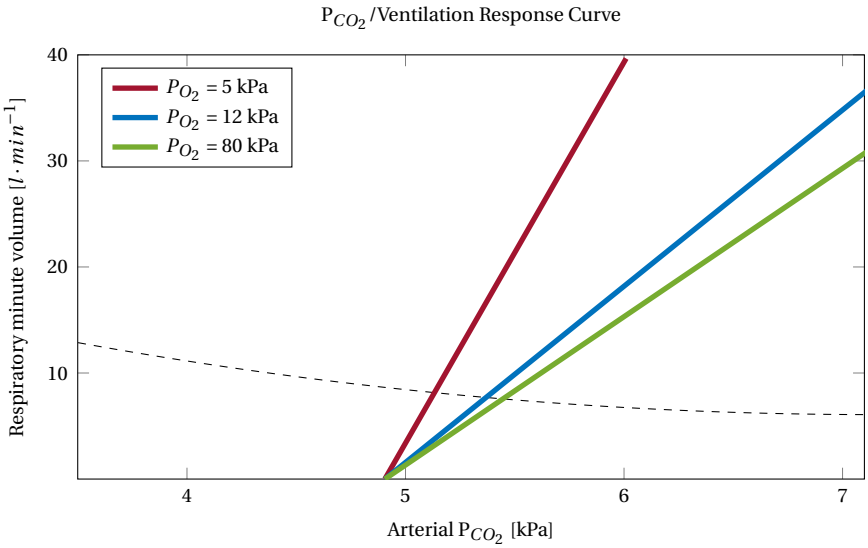

Figure 2.2: *Stylistic P_{CO_2}/ventilation response curve for three different situations of arterial P_{O_2}. Drawn with inspiration from [Lumb, 2010].*

2.2 Respiratory Depression

Most anesthesia and analgesia have an effect on the chemical and metabolic control of respiration [Dahan & Teppema, 2003]. The drug administration to patients undergoing surgery is in focus due to this effect. This section will discuss the respiratory depression caused by anesthesia and analgesia, as these drugs can still be found in patients in the postoperative period.

2.2.1 The Effect of Opioids on Respiration

The respiratory response to changes in P_aCO_2 (the central drive, D_c) in non medicated healthy people is generally more important than the response to changes in P_aO_2 (the peripheral drive, D_p) [Francisco, 2007]. When medicated, the brain's respiratory response to a change in P_aO_2 can be depressed resulting in low activation of the lung musculature. In general, opioids decrease the respiratory frequency and tidal volume through several mechanisms originated from various anatomical locations [Bailey, 1996]. The opioids are binding at the ventral surface of the medulla resulting in a blunted central respiratory drive response to changes in P_aCO_2 [Bailey, 1996]. The reduced central drive makes patients dependent on the peripheral drive to maintain an adequate respiration. The depression of D_c are dose-dependent for all μ-receptor agonists like morphine and fentanyl [Bailey, 1996].

The peripheral drive D_p can likewise be depressed by opioids. When D_p is depressed, the respiratory response to hypoxemia is reduced, which can be fatal to a non-monitored patient [Bailey, 1996]. The total depression of the respiratory drive to breath in terms of the P_aCO_2/ventilation response curve, described in Section 2.1.1.1, can be seen as a depression and right-shift of the response slope meaning a low sensitivity to changes in P_aCO_2 and risk of hypercarbia.

Both epidural and intrathecal opioids can lead to a delayed respiratory depression with peak depression 4-8 hours after administration and can depress respiration in up to 24 hours [Bailey, 1996]. This implies the importance of patient monitoring to avoid hypoxemia.

Opioids can furthermore be used to increase the respiration in patients suffering from thoracic or abdominal pain [Bailey, 1996; Francisco, 2007]. Analgesia can in these patients contribute to increased tidal volume, lung volume, stabilizing respiratory rate, cough and result in improved gas exchange [Bailey, 1996].

2.2.2 Postoperative Respiratory Depression

All patients undergoing surgery with anesthesia are in risk of developing postoperative respiratory depression [Dahan & Teppema, 2003]. Patients with impaired respiratory drive, sleeping disorders, COPD, neurological disorders and patients being female, elderly, hypo-ventilating or obese are in higher risk of developing respiratory depression when getting administered opioids and anesthesia [Dahan & Teppema, 2003; Francisco, 2007]. Postoperative hypoxemia can e.g. be caused by delayed wound healing, wound infection, myocardial ischemia, tachycardia and acute cognitive disturbances [Dahan & Teppema, 2003].

Out of the total amount of adverse drug events, respiratory events are only contributing with as little as 0.5-1.2%, but are represent in 12.3% of life threatening drug-induced diseases and furthermore 25-30% of the drug-induced deaths [Francisco, 2007]. These numbers emphasize how critical the condition of impaired respiration can be despite the relative low prevalence.

Most experimental studies of respiratory response of medicine are based upon measurements on healthy volunteers affected by only the one tested medication Dahan & Teppema [2003]. The effect of combined medications is often not studied Dahan & Teppema [2003], which can complicate the administration of anesthesia in premedicated patients, who often are stressed by multiple conditions and medications.

Sleep and especially REM-sleep can contribute to a decreased respiration and a decreased response to hypercarbia [Bailey, 1996], which furthermore is increasing the respiratory depression. When sleeping and during anesthesia, the wakefulness drive to breathe (D_w) is de-

creased [Duffin, 2005]. Impaired breathing during sleep is a common condition, why special attention is required to these patients to avoid hypoxemia [Dahan & Teppema, 2003].

Hypoxemia caused by respiratory depression can be developed up to five days postoperative with highest risk 2-3 days postoperative [Bailey, 1996; Hedenstierna, 2012; Rosenberg et al., 1994].

COPD patients do often have an impaired central respiratory drive because of a long term increased P_aCO_2, see Section 2.3. Because of the increased P_aCO_2 they are dependent on their peripheral drive to breath, and therefore oxygen treatment can be dangerous and in worst case result in apnoea [Francisco, 2007; Lumb, 2010].

2.2.3 Treatment of Respiratory Depression

Opioid induced respiratory depression can easily be treated, but the challenge lies in detecting patients in risk in time. The depression is not dangerous if detected within the first minutes, but 5-10 minutes with severe hypoxemia can cause irreversible nerve damage [Bailey, 1996]. By monitoring respiration, pupillary constriction, level of sedation and gas exchange, the patients in risk can be identified [Francisco, 2007]. Verbal and tactile stimulation or oxygen treatment administered in nasal catheter are sufficient treatment to avoid hypoxemia in most patients [Bailey, 1996]. In patients with severe respiratory depressions and especially respiratory acidosis or apnoea, additional treatment is necessary.

Naloxane is the most frequent used medicine to treat respiratory depression, and even small doses help patients with spontaneous breathing. If administered in larger doses, naloxane can contribute to higher risk of hypertension, stroke and pulmonary oedema, why respiratory depression must be treated with care and sufficient monitoring [Bailey, 1996], but new methods to describe respiration would be useful to provide better care [Francisco, 2007].

2.3 Respiratory Response in COPD patients

As with patients who are under the influence of opioids, patients with COPD can suffer from decreased central drive response [Bailey, 1996; Larraza et al., 2015b]. The central drive response is reduced due to high arterial Base Excess (BE) and HCO_3^- [Larraza et al., 2015b]. The increased HCO_3^- concentration alters the bicarbonate buffering system thereby making patients with COPD less responsive to changes in CO_2 and in some cases leaving only the peripheral chemoreceptor in control of the breathing [Lumb, 2010]. If the central drive is impaired in such a way that only the peripheral drive is controlling the patients breathing, oxygen treatment may pose a threat to the patient. Elevating inspired oxygen could cause the patient to lower or even stop breathing and hence cause hypercapnia [Lumb, 2010].

2.4 Summary

The respiration in healthy people is controlled by chemorereflexes, which respond to changes in P_aCO_2 and P_aO_2. The central drive to breathe (hypercarbia sensitive) is the primary drive to breathe. Patients with depressed central drive caused by e.g. opioids or COPD are dependent on their peripheral drive, why they are more susceptible of developing hypoxamia. New methods to estimate respiratory drive parameters is of clinical value when identifying patients in risk of developing hypoxamia and when aiding optimal respiratory treatment [Larraza et al., 2015a,b].

On this basis the following will describe an already existing model of the respiratory drive response in order to find out whether or not this model can be used when describing patients peripheral respiratory drive.

PART II

METHODS

CHAPTER 3

Description of the Respiratory Control Model

The following chapter will describe the physiologic model that will be used throughout the project. The model will be referred to as the "RDRIVE model".

The RDRIVE model uses input parameters estimated by a decision support system (DSS) called INVENT [Larraza et al., 2014]. INVENT is developed as a model-based DSS for selecting optimal ventilator settings [Rees, 2011].

The RDRIVE model consists of six mathematical model components. These six models respectively describes:

- Ventilation and pulmonary gas exchange
- Oxygenation and acid-base status of blood
- Acid-base status of CSF
- Cardiac output, arterial and mixed venous pools
- Interstitial fluid, tissue buffering and metabolism
- Chemoreflex respiratory control

In Figure 3.1 an abstract model of the set of models is presented. The gray boxes in Figure 3.1 show measured data, available from clinical measurements. This data is obtained from measurement of the pulmonary gas exchange and measurement of arterial blood gas [Larraza et al., 2015b]. Parameters written in the circles and square rectangular boxes with white background in Figure 3.1 are estimated by the model.

Figure 3.1 shows the four models, marked with green, that is used and described in this thesis. This includes a model describing pulmonary gas exchange, a model describing the blood acid-base compartment, a model describing the CSF acid-base compartment and lastly the respiratory drive model, which all individually contributes to the control of respiration. This chapter aims to give an introduction to each of these components and explain why they are included in the RDRIVE model.

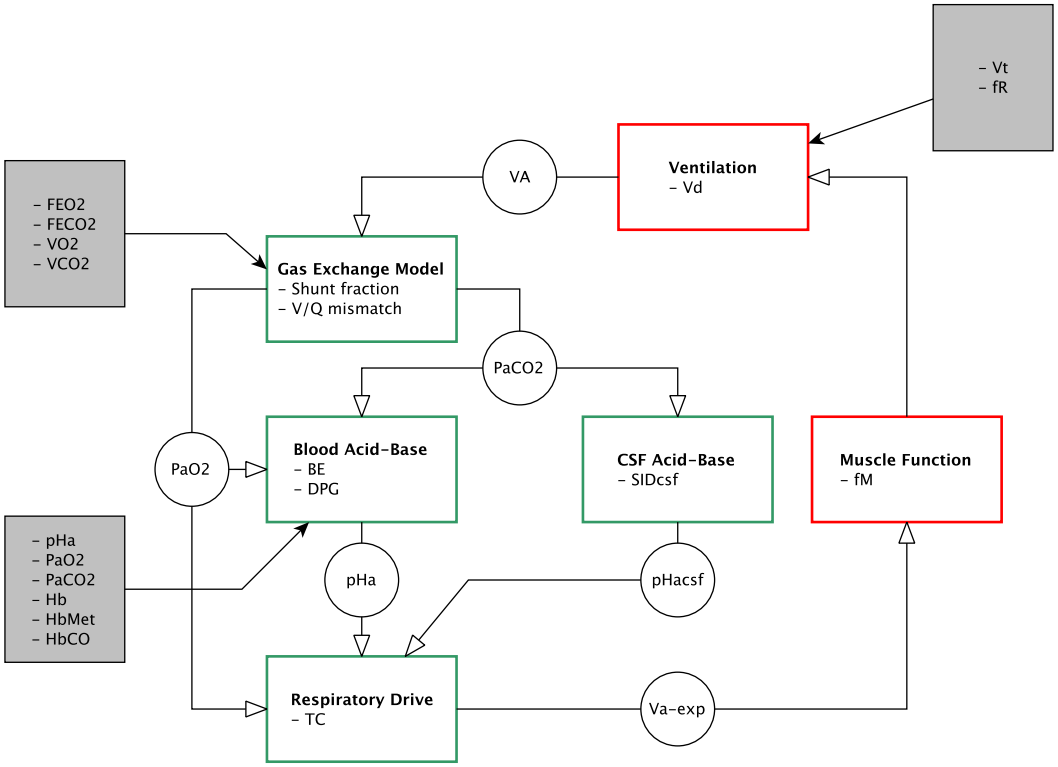

Figure 3.1: *The structure of the mathematical model used to parameterize the respiratory drive. The diagram is drawn with inspiration from [Larraza et al., 2015b].*

3.1 Ventilation and Pulmonary Gas Exchange

The first sub-model represents pulmonary gas exchange, see Figure 3.1. Gas exchange is modeled using three compartments, of which one is describing non-ventilated blood (pulmonary shunt) where no gas exchange occurs. The other two compartments are both ventilated and perfused and they are representing the gas exchange between alveoli and capillaries. This three compartmental model is shown in Figure 3.2.

Using the three compartments, an estimation of the match/mismatch in the ventilation/perfusion ratio and the fraction of shunted blood can be calculated. The input data used in the model are arterial blood saturation measured with pulse oximetry and several gas volumes sampled with a gas analyzer [Thomsen et al., 2014].

The model of ventilation and pulmonary gas exchange, represented by Equation 3.1, estimates the two parameters P_aO_2 and P_aCO_2. The relationship between P_aO_2 and P_aCO_2 and fraction of expired O_2 ($F_{et}O_2$) and CO_2 ($F_{et}CO_2$) [Karbing et al., 2011; Kjærgaard et al., 2003; Larraza et al., 2015b].

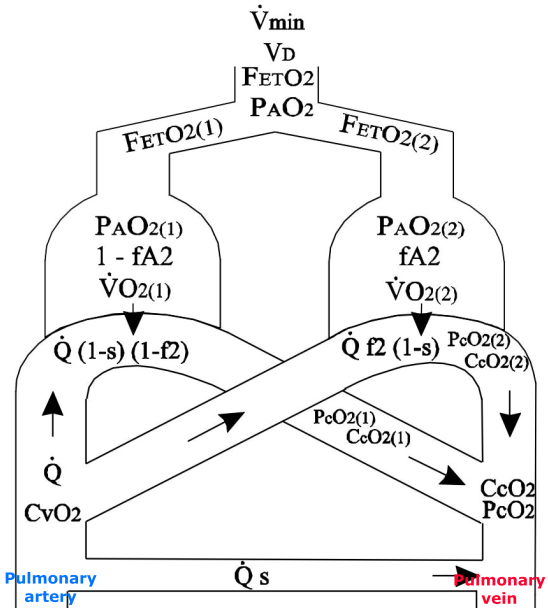

Figure 3.2: *Overview of the three compartmental model used in ALPE. Redrawn from [Larraza et al., 2014].*

$$P_aO_2,\, P_aCO_2 = \text{gas exchange}(F_{et}O_2,\, F_{et}CO_2) \tag{3.1}$$

A way to use the gas exchange model is in the clinical bedside tool "Automatic Lung Parameter Estimator" (ALPE) [Rees et al., 2002]. This tool parameterizes gas exchange, by estimating high and low ventilation/perfusion mismatch and shunt fraction [Rees et al., 2002; Thomsen et al., 2013]. This parameterization is done by varying F_iO_2 in 3-5 steps, and measuring S_pO_2 and $F_{et}O_2$ in each step when steady state levels are reached [Thomsen et al., 2013]. The measurements can then be used to estimate the pulmonary gas exchange parameters. The fundamental assumption in this model is a state of equilibrium between alveolar and capillary gases. The main output of the gas exchange model is an estimation of pulmonary shunt and ventilation/perfusion ratio. This sub-model is well-documented and has previously been tested in clinical settings [Karbing et al., 2011, 2007; Thomsen et al., 2014].

3.2 Oxygenation and Blood Acid-Base Status

The second sub-model is used to simulate the acid-base chemistry of blood, see the "Blood Acid-Base" box in Figure 3.1. This model is based upon the mixing of venous blood with blood with elevated O_2 and reduced CO_2 levels [Rees et al., 2010]. The mixing of blood with different O_2 and CO_2 levels is in normal conditions happening, when shunted pulmonary blood mixes with lung capillary blood [Rees et al., 2002].

This mathematical model of acid-base chemistry of blood is based upon a system of 28 equations which are formulated by considering mass action[1] and mass balance[2]. These equations are solved simultaneously using six variables. The six variables are each representing a blood component [Rees & Andreasen, 2005; Rees et al., 2010]:

- Carbon dioxide (CO_2)
- SID (Strong Ion Difference - Buffer Base)
- Hemoglobin in erythrocytes ($Hb(RH)_bNH_3^+$)
- A_{tot} (weak acid)
- Oxygen (O_2)
- 2,3-diphoshoglycerate (DPG)

The model includes the acid-base and oxygenation of red blood cells along with the binding of O_2, CO_2 and H^+ ions on hemoglobin, which previous physiological blood status models described by Siggaard-Andersen, 1974; Stewart, 1983 and Siggaard-Andersen et al., 1988 do not include.

The chemical reactions shown in Equation 3.2 describe, that CO_2 can react with water to form bicarbonate (HCO_3^-) and hydrogen ions (H^+):

$$H^+ + HCO_3^- \leftrightharpoons H_2O + CO_2 \tag{3.2}$$

This reaction describes how the pH-status in blood changes due to the level of CO_2 in the blood.

In general, the model describes the relationship between P_aO_2, P_aCO_2, oxygenation and acid-base status, which is represented by Equation 3.3 [Larraza et al., 2015b].

$$pHa,\, S_aO_2 = \text{blood acid base}(P_aO_2,\, P_aCO_2) \tag{3.3}$$

Using pHa, P_aO_2, P_aCO_2, S_aO_2, bicarbonate concentration (HCO_3^-) and hemoglobin concentrations taken from a measurement of arterial blood gas, and measured values of $\dot{V}O_2$ and $\dot{V}CO_2$, the model is tuned to the individual patient [Larraza et al., 2015b]. The values for P_aO_2 and P_aCO_2 can be estimated from the gas exchange model, see Equation 3.1.

To summarize the functionality of this part of the model, the acid-base status of blood needs to be estimated in order to calculate the acid-base status of CSF and hereby the resulting influence on the respiratory chemoreceptors.

[1] Prediction of behavior of solutions in dynamic equilibrium.
[2] Conservation of mass in a system.

3.3 Acid-Base Status of Cerebral Spinal Fluid

The CSF acid-base status, see Figure 3.1, is based upon the cerebrospinal fluid acid-base model presented by Duffin, 2005. The model describes the relation between CSF acid-base status and PCO_2. The P_{CO_2} in CSF is equivalent to arterial P_{CO_2}, when brain produced CO_2 is added [Duffin, 2005].

In total, seven equations are used to describe the model of CSF acid-base. These equations are solved simultaneously, in order to estimate the strong ion difference (SID) in CSF (SID_{csf}). The estimated value is assumed to be constant due to the blood-brain barrier's ability of constraining the ion exchange [Larraza et al., 2014].

The model can deal with altering base excess (BE) describing metabolic acidosis[3] or metabolic alkalosis[4] [Larraza et al., 2014]. The estimation of SID_{csf} allows simulation of the alterations in the central chemoreceptor signaling $[H^+_{csf}]$ and thereby changes to the respiratory drive [Larraza et al., 2014].

The model describing CSF acid-base status and P_aCO_2 can be described as Equation 3.4. The model is tuned to the patient using P_aCO_2 from a ABG [Larraza et al., 2015b]. From P_aCO_2 the SID_{csf} can be calculated.

$$pH_{csf} = \text{CSF acid base}(P_aCO_2) \tag{3.4}$$

This sub-model is included to model how changes in ion concentrations in the CSF affects the respiratory center and the following respiratory response. The respiratory response is further described in Section 3.4.

3.4 Chemoreflex Respiratory Control

The last of the sub-models described in this project is the model of respiratory control ("Respiratory Drive" in Figure 3.1). The respiratory control and respiratory drive can be described by the following seven parameters besides $[H^+_a]$ and $[H^+_{csf}]$, Larraza et al. [2014]:

The respiratory drive, and hereby the alveolar ventilation ($\dot{V}A$) and total drive to breathe, is the sum of the three drives D_p, D_c and D_w, [Duffin, 2005], see Equation 3.5.

$$\dot{V}A = D_p + D_c + D_w \tag{3.5}$$

D_p is the respiratory drive contribution from the peripheral chemoreceptors and is described by a linear function of the difference between the peripheral chemoreceptor threshold (T_p) and the arterial

[3] Reduced bicarbonate and base excess.

[4] Increased bicarbonate and base excess.

Symbol	Name	Normal Value	Unit
D_p	Peripheral drive	N/A	$l \cdot min^{-1}$
D_c	Central drive	N/A	$l \cdot min^{-1}$
D_w	Wakefulness drive	2 - 7	$l \cdot min^{-1}$
S_p	Peripheral chemoreceptor sensitivity	0.29	$l \cdot min^{-1}(nmol \cdot l^{-1})$
S_c	Central chemoreceptor sensitivity	1.78	$l \cdot min^{-1}(nmol \cdot l^{-1})$
T_p	Peripheral chemoreceptor threshold	37.75	$nmol \cdot l^{-1}$
T_c	Central chemoreceptor threshold	45.24	$nmol \cdot l^{-1}$

Table 3.1: *Parameters and constants used in the chemoreflex respiratory control model Duffin [2005]; Larraza et al. [2014].*

hydrogen ion concentration $[H_a^+]$, [Duffin, 2005; Larraza et al., 2014], see Equation 3.6.

$$D_p = S_p([H_a^+] - T_p), \text{ if } D_p < -1 \text{ then } D_p = -1 \tag{3.6}$$

The sensitivity of the peripheral chemoreceptors S_p is equal to the slope of this linear function. If D_p is below -1 it is determined to be equal to -1 because the drive is limited to only add a small depression to $\dot{V}A$. The logic behind using a negative value of D_p is to model apnoea if both D_p and D_c is depressed Larraza et al. [2014].

D_c is likewise the respiratory drive contribution from the central chemoreceptors located in the medulla. D_c is a linear function determined by the difference between the central chemoreceptor threshold (T_c) and the CSF hydrogen ion concentration $[H_{csf}^+]$, see Equation 3.7 [Duffin, 2005; Larraza et al., 2014].

$$D_c = S_c([H_{csf}^+] - T_c), \text{ if } D_c < -1 \text{ then } D_c = -1 \tag{3.7}$$

The sensitivity of the central chemoreceptors S_c is equal to the slope of the linear function. If D_c is below -1 it is determined to be equal to -1 because the drive is limited to only add a small depression to $\dot{V}A$. The logic behind using a negative value of D_p is to model apnoea if both D_p and D_c is depressed Larraza et al. [2014].

The mathematical model of the respiratory drive is used to estimate T_c, that being the threshold for which the concentration of hydrogen ion in CSF affects the central drive and thereby the ventilation [Larraza et al., 2015b]. This model is tuned using pH_a from a ABG, $\dot{V}O_2$ and $\dot{V}CO_2$.
The respiratory drive model is described by Equation 3.8.

$$\dot{V}A_{exp} = \text{respiratory drive}(P_aO_2, pH_a, pH_{csf}) \tag{3.8}$$

D_w is the third contribution to $\dot{V}A$, as described in Equation 3.5. D_w is the wakefulness drive, which represent the behavioral component of breathing and is thereby considered independent of the D_c and D_p. When unconscious, the D_w is equal to zero contribution to the drive to breathe. The normal value of D_w in a healthy person is by Duffin, 2005 described to be 7 $l \cdot min^{-1}$ (minute volume). In this model, the normal value of D_w is determined to be 2 $l \cdot min^{-1}$ ($\dot{V}A$) indicating that D_w is not the drive with most contribution to ventilation in patients during mechanical ventilation to whom the model is originally designed to [Larraza et al., 2014].

3.5 Usage of The Model

The model estimates the value for T_c by numerical optimization. This optimization process simultaneously solves the four models described by equations: 3.1, 3.2, 3.4 and 3.8.
As described, the model uses measured inputs from the ALPE measurement (describing pulmonary gas exchange) and arterial blood gas. During the optimization a value of pH_a is estimated by the model and the difference between this simulated value of pH_a and the measured value of pH_a from the ABG is minimized [Larraza et al., 2015b].
When the numerical optimization is completed the estimated values for the central respiratory drive can be used, when simulating change in ventilator treatment [Larraza et al., 2015b].

The RDRIVE model in its current state is not designed to estimate the parameters describing the patient's peripheral respiratory drive. Therefore, this thesis aims to develop a simple method for estimation of the parameters that are involved in describing the peripheral drive.

CHAPTER 4

Peripheral Drive Modeling

This chapter will examine whether the estimation of peripheral drive in the RDRIVE model adequately describes the total drive to breathe.

An overview of the methods used throughout this thesis is shown in Figure 4.1, where the final model is representing a new method for parametrization of the peripheral drive.

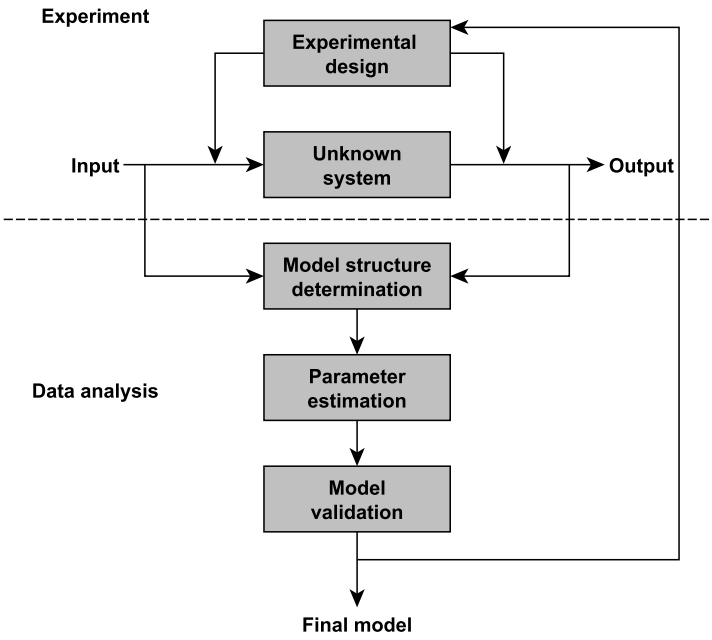

Figure 4.1: *Methods used to model respiratory peripheral drive parameters. Adapted from [Cobelli & Carson, 2008].*

The peripheral chemoreflex model is representing the underlying physiology and the included parameters can be directly related to physiological parameters in theory. On this basis the modeling of the peripheral drive will include the model equations and parameters previously described in Section 3.4. The concept of Figure 4.1 is that the model development is an iterative process, where the model output continuously gets compared with the real system output in order to change the model structure to best fit experimental data.

The elements in Figure 4.1 represent three parts in the model procedure [Cobelli & Carson, 2008]:

- Model formulation
- Model identification
- Model validation

The model formulation will provide a more detailed description of the peripheral drive model and a specification of the relationship between parameters and variables.

The model identification will specify the structure of the model and examine the unknown parameters which needs to be considered before the model can be completed. The identification process will be performed by using data from simulated experiments and noise-free data obtained from the literature. The goal of this section is to address whether the experimental data is sufficient to estimate all unknown parameters or if the model complexity is too high [Cobelli & Carson, 2008].

The model validation represents the results of the parameter estimation. This part will examine whether the model is sufficiently descriptive for the intended purpose of describing peripheral drive in spontaneously breathing patients.

For the ease of reading, the method of estimating the parameters in the peripheral drive will be described as the "O2-RDRIVE model" throughout this thesis.

CHAPTER 5

Model Formulation

It is important to consider that the degree of complexity in the mathematical formulation of the model needs to be consistent with the intended purpose of the model [Cobelli & Carson, 2008]. The O2-RDRIVE is a sub-model of the comprehensive full body RDRIVE model. The models are a conceptual representation of the underlying physiology based upon the methods and assumptions described in Chapter 3. Hereby it is clearly stated, that the mathematical model is an approximation of the underlying physiological system, where e.g. the respiratory chemoreflex response of man is assumed to be as described in the literature by Duffin and Larraza et al..

As discussed in Section 3.4, the peripheral drive is dependent on the parameters $Po2$, A and T_p, which all are modeled as constants in the RDRIVE model, [Larraza et al., 2014], see equations Equation 5.1 and Equation 5.2.

$$S_p = \frac{A}{P_aO_2 - Po2} \tag{5.1}$$

where S_p is the peripheral drive sensitivity to oxygen and P_aO_2 is the arterial oxygen pressure. The value of $Po2$ in Equation 5.1 is referred to as "*the oxygen pressure for maximum sensitivity before failure*" [Duffin, 2005]. A is an area constant for the relation between S_p and P_aO_2. The peripheral drive is, in terms of $[H_a^+]$ estimated with Equation 5.2.

$$D_p = S_p([H_a^+] - T_p) \tag{5.2}$$

where $[H_a^+]$ is the blood hydrogen concentration, which is estimated by the RDRIVE model. T_p is the peripheral chemoreceptor threshold. The constant values used in the RDRIVE model for the parameters $Po2$, A and T_p are originally described by Duffin, 2005 and can be seen in Table 5.1:

Symbol	Description	Normal Value	Unit
A	Area constant	2.33	$\mathrm{l} \cdot \mathrm{kPa}\ (\mathrm{min} \cdot \mathrm{nM} \cdot \mathrm{l}^{-1})^{-1}$
$Po2$	Maximum oxygen sensitivity	4.00	kPa
T_p	Peripheral chemoreceptor threshold	37.75	$\mathrm{nmol} \cdot \mathrm{l}^{-1}$

Table 5.1: *Normal values for peripheral drive parameters used in the RDRIVE model.*

The two equations, 5.1 and 5.2, represent the mathematical representation of the conceptual model of the peripheral drive. In order to investigate how well this simplification of the respiratory system describes patient data, the model will be evaluated with noise-free and noise polluted simulated data, see Section 6.3 and patient data, Chapter 7. The individual model parameters will identified in the following chapter Chapter 6.

CHAPTER 6

Model Identification

Preliminary analysis of the RDRIVE model's ability to describe peripheral drive in spontaneously breathing patients has shown that the model does not adequately describe the peripheral drive for some patients with depressed central drive. Therefore, the peripheral drive response to changes in the three model parameters $Po2$, A and T_p will now be examined by performing simulated experiments with the model equations Equation 5.1 and Equation 5.2. The goal of the experiments is to identify which parameters are most important in the model, which will be further discussed in Section 6.1.

The alveolar ventilation for a simulated healthy patient is estimated with the RDRIVE model using the normal values as shown in Table 5.1. The simulations are performed as experiments, where the inspired oxygen fraction is changed to examine the ventilatory response. The following three figures will illustrate how the parameters individually affect the drive when simulating changes in arterial oxygen pressure, see Figure 6.1, Figure 6.2 and Figure 6.3. The blood parameters pH, BE and SID_{csf} are held constant during the simulations, as it is assumed that these parameters do not change when changing the inspired oxygen in a short period [Larraza et al., 2014]. As these values are held constant the central drive is also assumed not to change.

As seen in Figure 6.1, the sensitivity of D_p is decreased with a lower value of $Po2$ while D_p is highly increased by a higher value of $Po2$. This relationship is expected because as seen in Equation 5.1, an increase in $Po2$ will reduce S_p and vice versa.

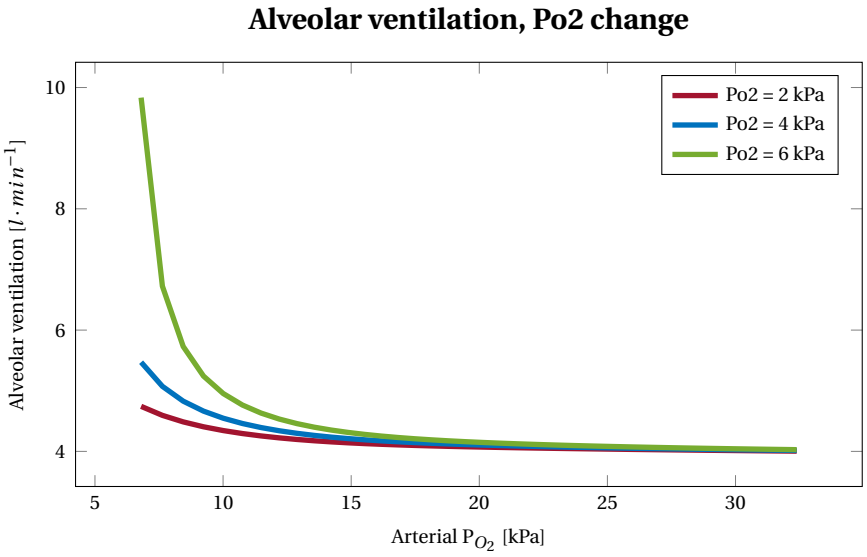

Figure 6.1: *Experiment of peripheral drive sensitivity to changes in Po2 in a healthy person. Data is simulated. The blue line represent the original RDRIVE response. A and T_p are set to normal values as shown in Table 5.1.*

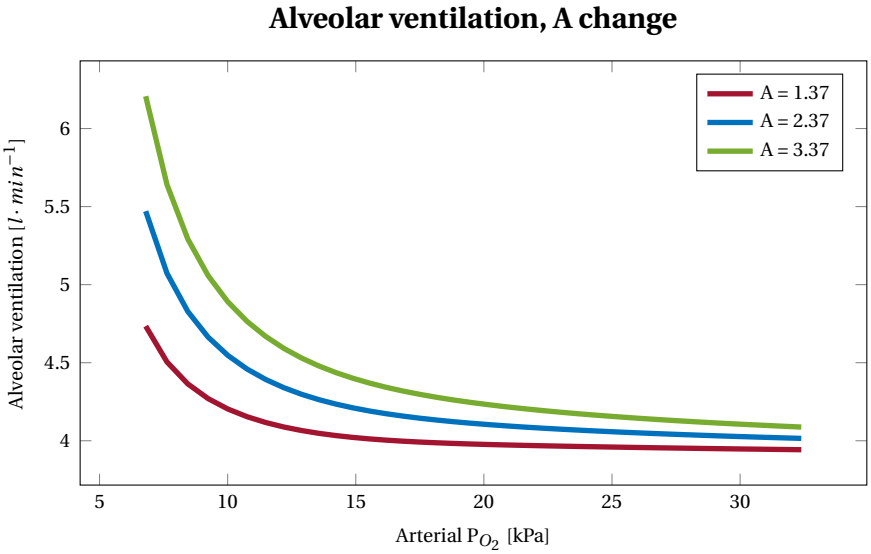

Figure 6.2: *Experiment of peripheral drive sensitivity to changes in A in a healthy person. Data is simulated. The blue line represent the original RDRIVE response. Po2 and T_p are set to normal values as shown in Table 5.1.*

Figure 6.2 shows how $\dot{V}A$ is increased by an increase in A and decreased by a decrease in A much like the response by changes in $Po2$.

In Figure 6.3 it is shown that $\dot{V}A$ is decreased by an increase in the value of T_p while $\dot{V}A$ is increased by a decrease in T_p.

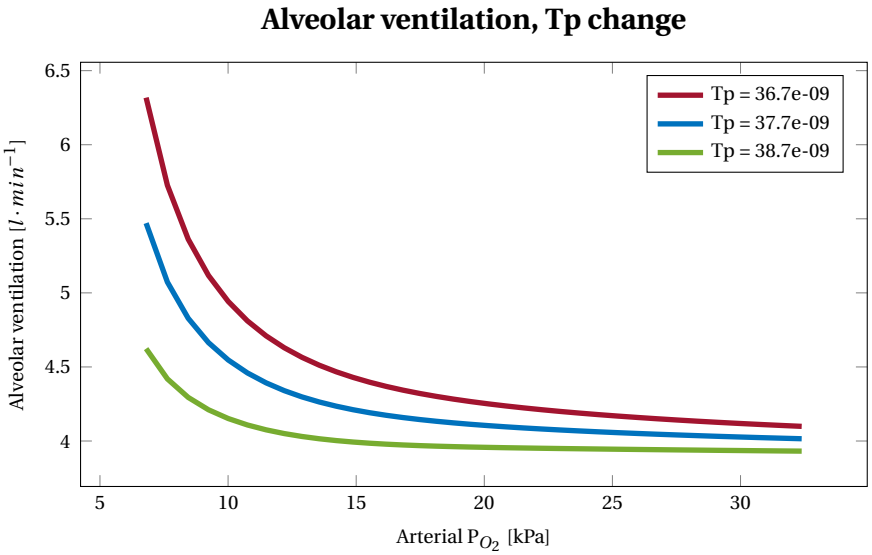

Figure 6.3: *Experiment of peripheral drive sensitivity to changes in T_p in a healthy person. Data is simulated. The blue line represent the original RDRIVE response. Po2 and A are set to normal values as shown in Table 5.1.*

The above experiments clearly states that D_p is dependent on the parameters $Po2$, A and T_p in a simulated healthy person. By inspection of the respiratory responses of the three experiments, one would suspect, that the three parameters are not all needed to describe the peripheral drive adequately. This leads to the definition of the identifiability problem, which will be presented in the following section.

6.1 The Identifiability Problem

Is it theoretical possible to uniquely estimate all unknown parameters in a mathematical model? If all data is complete and noise-free this would not be a problem, [Cobelli & Carson, 2008]. In this model however the test data is not noise-free and there are (at least) three unknown parameters in the sub-model, which are simplified by the two peripheral drive equations Equation 5.1 and Equation 5.2. There exists two solutions to this dilemma, either reduce the complexity of the model or add additional measurement data [Cobelli & Carson, 2008]. The latter solution implies that additional measured variables are required to provide more accurate estimations of the unknown parameters. As the RDRIVE model is thought of to be a simple clinical bedside tool [Larraza et al., 2015a,b], which also applies for the O2-RDRIVE model. On this basis no additional measurements are wanted as these will complicate the usability.

The identifiability problem is addressed in the formulation and identification part of the modeling strategy to test if the proposed model can describe ideal and noise-free data [Cobelli & Carson, 2008]. The

model will be tested on noise-free data in Section 6.3. If the model can not describe ideal data, there is no possibility that the model can describe real data [Cobelli & Carson, 2008].

Before the model is tested, the unknown parameters will be identified to ensure, that they can be uniquely identified. The peripheral drive sensitivity is described by the following equation, where the parameters A and $Po2$ are replaced by the parameters P_1 and P_2 in order to simplify the expression, see Equation 6.1.

$$S_p(P_aO_2) = \frac{A}{P_aO_2 - Po2} = \frac{P_1}{P_aO_2 - P_2} \tag{6.1}$$

The relation between the peripheral drive and the drive sensitivity is shown in Equation 6.2.

$$D_p(P_aO_2) = S_p(P_aO_2) \cdot (H^+ - T_p) \cdot 10^9 \tag{6.2}$$

H^+ is a patient specific estimation of arterial hydrogen ion concentration, which is assumed not to change between the ALPE measurements, why it will be replaced by the constant K. T_p is the third unknown parameter, which will be denoted P_3, see Equation 6.3.

$$D_p(P_aO_2) = S_p(P_aO_2) \cdot (K - P_3) \cdot 10^9 \tag{6.3}$$

$$\hat{P}_3 = (K - P_3) \cdot 10^9 \tag{6.4}$$

By inspection of the P_3 parameter, it is only dependent on K and the scalar 10^9, why it can be represented by the parameter $\hat{P}_3$, see Equation 6.4. The boundaries for which this is true is described in Table 6.1. By using this notation, the drive equation can be rewritten as:

$$D_p(P_aO_2) = S_p(P_aO_2) \cdot \hat{P}_3 = \frac{P_1 \cdot \hat{P}_3}{P_aO_2 - P_2} \tag{6.5}$$

The drive is now expressed in terms of the parameters P_1, P_2 and $\hat{P}_3$. However it is easily seen, that it is not possible to obtain an unique solution for the unknown parameters P_1 and $\hat{P}_3$. Hence, they are interchangeable and each of the two parameters has two solutions to the same output.

When returning to the original expression of the drive equations, the above analysis states that either A or T_p should be held constant during the parameter estimation in order to provide unique patient specific parameters.

Parameter Boundaries

By inspection of the drive equations Equation 5.1 and Equation 5.2, the parameter boundaries will now be analyzed for where each of the three unknown parameters gives most physiological sense.

The lower boundary for $Po2$ is set to be $\approx$ 0 kPa, which ensures that $Po2$ can always take values below P_aO_2 - a requirement for the RDRIVE model not to fail. The upper boundary is set to be no higher than the P_aO_2. The upper boundary ensures that the peripheral drive sensitivity is not negative. The A parameter is an area constant for the relation between S_p and P_aO_2, and is empirical chosen to be studied in the interval from 1 to 50. In order to provide a physiological meaningful drive estimation, the value of T_p should be lower than the patient specific $[H_a^+]$, because it represents a threshold value for when the peripheral drive should increase. The lower boundary is empirically chosen, see Table 6.1.

Parameter	Unit	Lower boundary	Upper boundary
A	$[\mathrm{l} \cdot \mathrm{kPa}\ (\mathrm{min} \cdot \mathrm{nM} \cdot \mathrm{l}^{-1})^{-1}]$	1	50
$Po2$	[kPa]	≈ 0	P_aO_2
T_p	[nmol/l]	30	$[H_a^+]$

Table 6.1: *Physiological meaningful limits for the three unknown peripheral drive parameters.*

With this knowledge in mind, the parameter estimation methods will be discussed in the following section.

6.2 Parameter Estimation Methods

The goal of using the O2-RDRIVE model is to describe the specific patients' peripheral drive parameters. The parameters used to describe D_p are in the RDRIVE-model assumed to be constant in the estimation of the central drive. To better describe the respiratory drive in patients with spontaneous breathing, the parameters describing D_p must be assumed not to be the same for every person. Hereby (some of) the unknown parameters A, T_p and $Po2$ must be estimated to the individual patient to better describe its peripheral drive.

Figure 6.4 provides an overview of how the specific patient respiratory drive parameters will be estimated using the RDRIVE and O2-RDRIVE models.

First the central drive (D_c) needs to be estimated. This will be done using the RDRIVE-model. Using the RDRIVE model D_p is assumed to be constant. To minimize the possible bias this will have on the overall estimation of ventilation, the estimation of D_c will be performed to the highest available F_iO_2 measurement. At highest F_iO_2 the influ-

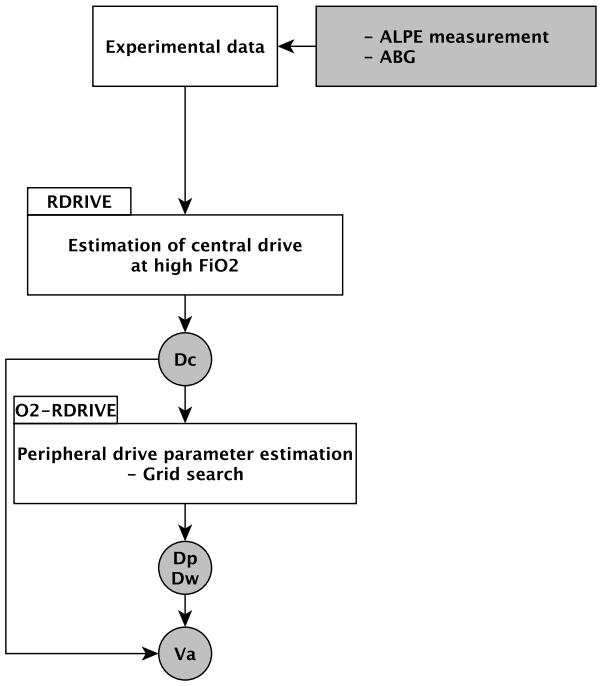

Figure 6.4: *Overview of the respiratory drive estimation using the O2-RDRIVE model. The methods are further described in the text.*

ence of D_p is assumed to be as low as possible, indicated by the red arrow in Figure 6.5.

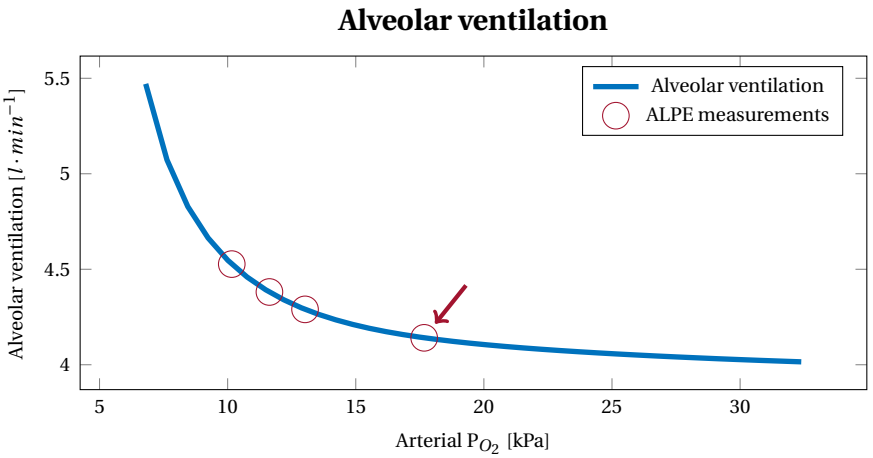

Figure 6.5: *Experiment of peripheral drive sensitivity in a simulated healthy patient. The red arrow marks a high value of oxygen pressure, where the D_p contribution to total ventilation is low compared to the measurements at low oxygen pressure marked by the red circles. The four red circles corresponds to $F_{et}O_2$ at 0.12, 0.14, 0.16 and 0.23.*

The alveolar ventilation simulation in Figure 6.5 is performed as an experiment, where the inspired oxygen fraction is changed. The red

circles in Figure 6.5 represent ALPE measurement points at $F_{et}O_2$ = 0.12, 0.14, 0.16 and 0.23 corresponding to the arterial P_{O_2} shown on the x-axis in the figure.

It is assumed that D_c is not dependent on F_iO_2, why it is assumed constant in the estimations of D_p parameters. As described by Duffin, 2005 D_w represents the drive to breath when awake, that can not be directly related to neither D_c or D_p. In this thesis, D_w is estimated as described in Section 6.4.

D_p can be estimated as in Equation 6.6.

$$D_p = \dot{\text{V}}\text{A} - D_c - D_w \tag{6.6}$$

The next step is to estimate the parameters A, T_p and $Po2$ using the drive equations 5.1 and 5.2.

The unknown parameters will be estimated by using a grid search method. Each parameter will be tested within the predefined interval, see table Table 6.1.

The parameters will be evaluated by the goodness of fit according to the weighed residual sum of squares (WRSS) between the measured ventilation to each of the 4-5 ALPE data points, y_i, and the estimated $\dot{\text{V}}\text{A}$ (the sum of the three drives) denoted by z_i. The error function is described in Equation 6.7.

$$\text{WRSS} = \sum_{i=1}^{N} w_i (z_i - y_i)^2 \tag{6.7}$$

where w_i symbolizes the weigh used at each observation i and N symbolizes the total number of observations. The observation at highest inspired oxygen fraction is believed to be more accurate. On this basis, WRSS will be calculated in two ways: In the first way the weigh at all points are equal. In the second way the weigh at the highest F_iO_2 is weighed five times higher than the other observations.

As earlier discussed, it is not preliminary known how many of the three unknown drive parameters that will best describe the patients seen from a physiological perspective. However, by the analysis of the identifiability problem in Section 6.1 it is decided not to include the parameter A in the grid search, hence it will be held constant at the original value proposed by Larraza et al. [2014], see Table 5.1.

The grid search method will be performed in five unique combinations of the unknown parameters set as either variable or constants:

- **Two parameter grid search**
  T_p and $Po2$: A is held constant
- **One parameter grid search**
  $Po2$: A and T_p are held constant
  T_p: A and $Po2$ are held constant
  T_p-strategy: T_p is estimated first and then held constant while estimating $Po2$
- **RDRIVE**
  RDRIVE: A, $Po2$ and T_p are held constant

Before testing the parameter estimation methods on patient data, the methods will be tested on noise-free data in the following section.

6.3 Parameter Estimation using Noise-Free Data

This section aims to test the O2-RDRIVE model's methods of parameter estimation as described in the section above. The tests will be done with the use of noise free data, which is generated by the RDRIVE model itself. Besides testing the methods on the noise free data, the methods will be tested on the same simulation data with respectively 3% and 5% added white noise (uncorrelated).
The O2-RDRIVE estimation methods will be tested both with and without weighing in the error function (see Equation 6.7), in order to compare the results with how the parametrization will be performed with the real data set in Chapter 7. The estimation methods are expected to provide an accuracy equivalent with the amplitude of added noise evaluated by their mean squared error accordingly.

In Table 6.2 the mean squared error between measured and estimated $\dot{V}A$ is listed. In Figure 6.6(a) the noise free data from the model is plotted along with the estimated $\dot{V}A$ produced by the five methods. As seen from the Table 6.2 and Figure 6.6(a) the estimated $\dot{V}A$ describes the simulated $\dot{V}A$ from the model adequately.

In Figure 6.6(b) random noise within 3% of the measured $\dot{V}A$ have been added to the noise free data from the RDRIVE model. This is done in order to test whether or not the parameter estimation methods of the O2-RDRIVE model are able to estimate $\dot{V}A$ in noise polluted data. As seen in Figure 6.6(b) all the estimation methods estimates an almost identical $\dot{V}A$ and none of the methods succeed in estimating an accurate $\dot{V}A$ at 0.14 and 0.16 $F_{et}O_2$.

The MSE between the original data and the 3% noise polluted data is: $10.1 \cdot 10^{-3}$ (l/min)^2. As seen in Table 6.2 the MSE between estimated $\dot{V}A$ for 3% noise polluted data and the simulated $\dot{V}A$ with no noise has a mean error for all methods of: $9.63 \cdot 10^{-3}$ (l/min)^2. This mean error

Estimation method	Constants	Noise free	3% noise	5% noise	5% noise and weighed
		MSE [(l/min)^2]			
RDRIVE	A, T_p, $Po2$	$6.93{\cdot}10^{-4}$	$9.66{\cdot}10^{-3}$	0.0903	0.0903
O2-RDRIVE. 1 param.	A, T_p	$1.33{\cdot}10^{-4}$	$9.65{\cdot}10^{-3}$	0.0564	0.0607
O2-RDRIVE. 1 param.	A, $Po2$	$2.13{\cdot}10^{-4}$	$9.63{\cdot}10^{-3}$	0.0576	0.0714
O2-RDRIVE. 2 param.	A	$0.91{\cdot}10^{-4}$	$9.56{\cdot}10^{-3}$	0.0564	0.0693
O2-RDRIVE. Tp-strategy	A	$2.03{\cdot}10^{-4}$	$9.63{\cdot}10^{-3}$	0.0575	0.0589
Mean Error All Methods		$2.66{\cdot}10^{-4}$	$9.63{\cdot}10^{-3}$	0.0636	0.0701

Table 6.2: *Parameter estimations using the four methods on noise free data and data with 3% and 5% added noise.*
MSE between simulated and 3% noise polluted data: $10.1{\cdot}10^{-3}$ (l/min)^2. MSE between simulated and 5% noise polluted data: 0.0956 (l/min)^2.

is almost identical to the MSE between simulated $\dot{V}A$ with no noise and simulated $\dot{V}A$ with 3% noise. This indicates that the five tested methods describes $\dot{V}A$ adequately in this evaluation.

The same trend is seen with parameter estimation at simulated data with 5% noise pollution. The MSE between estimated $\dot{V}A$ for 5% noise polluted data and the simulated $\dot{V}A$ with no noise has a mean error for all methods of: 0.0636 (l/min)^2. As in the evaluation above, this mean error is almost identical to the MSE between simulated $\dot{V}A$ with no noise and $\dot{V}A$ with 5% noise. This again indicates that the five tested methods describes $\dot{V}A$ adequately in this evaluation.

It should be noted, that the MSE listed for the noise polluted simulated data in Table 6.2 is between that data and the estimated $\dot{V}A$ - not between simulated data with no noise and estimated $\dot{V}A$.

The MSE for parameter estimation with the weighing is also listed in Table 6.2. The MSE is almost identical but though a bit larger, than the MSE obtained without the weighing. The weighing is though used throughout the results in Chapter 7, as this method is considered more physiological correct.

Table 6.2 shows that all the methods adequately estimates $\dot{V}A$ in the noise free data. The RDRIVE model is the only one of the five methods that has a conspicuous more inaccurate result in the other three data set, when noise is added. It is stated, that there is only a little difference in MSE between the estimation methods (with the O2-RDRIVE, however the parameters can only be related to the physiology if they can be uniquely identified for the specific patient. To analyze whether this is possible the error functions related to the shown MSEs in Table 6.2 will be presented in Figure 6.7, Figure 6.8, Figure 6.9 and Figure 6.10.

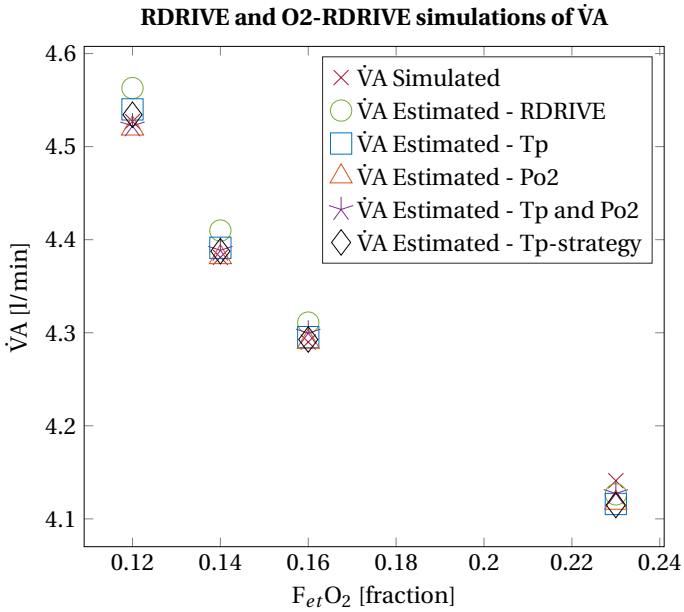

(a) *Noise free simulation data*

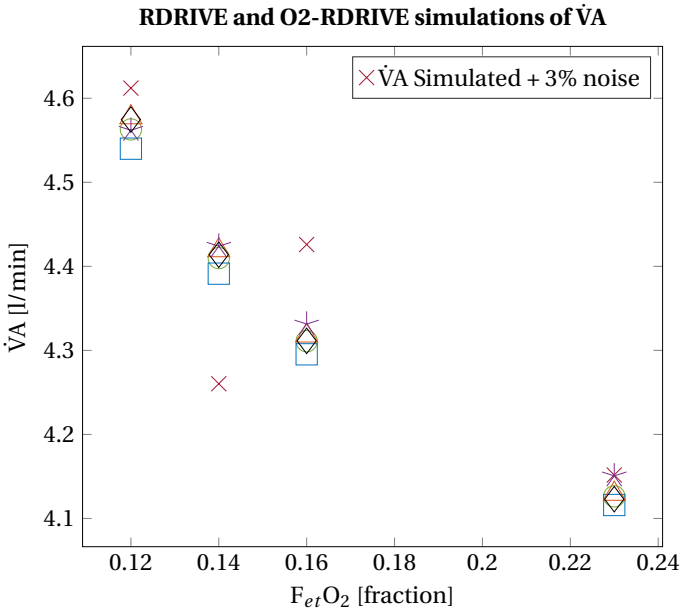

(b) *Simulation data with 3% added noise*

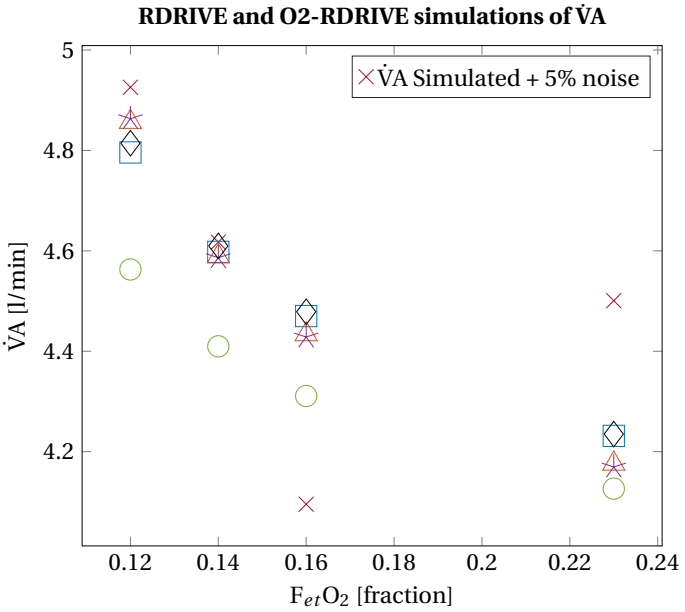

(c) *Simulation data with 5% added noise*

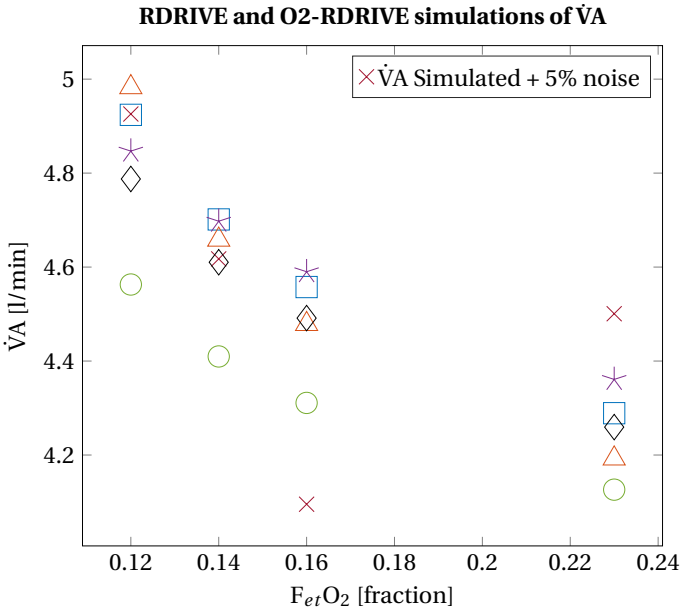

(d) *Simulation data with 5% added noise. The V̇A simulation at 0.23 $F_{et}O_2$ is weighed 5 times more*

Figure 6.6: *Peripheral drive parameter estimations using noise free and noise polluted data. The data is simulated with the RDRIVE model. Symbol explanation is placed in Figure 6.6(a). Notice that the V̇A from the RDRIVE simulation (green circles) is the same for the four tests.*

Figure 6.7 and Figure 6.8 show the error functions of the parameter estimations from Figure 6.6. The error functions of the T_p-estimations are shown in the left side figures (Figure 6.7(a), Figure 6.7(c), Figure 6.8(a) and Figure 6.8(c)). The T_p-estimations are in all four examples able to locate the global error minimum relatively close to the original T_p-value of 37.75 nmol$\cdot$ l^{-1} despite added noise.

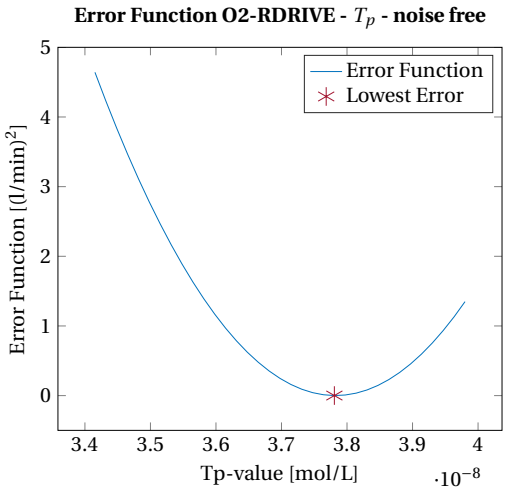

(a) *Error function. Estimation of T_p - noise free.*

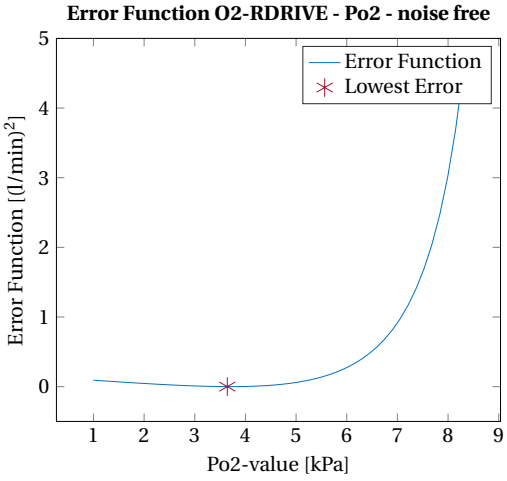

(b) *Error function. Estimation of Po2 - noise free.*

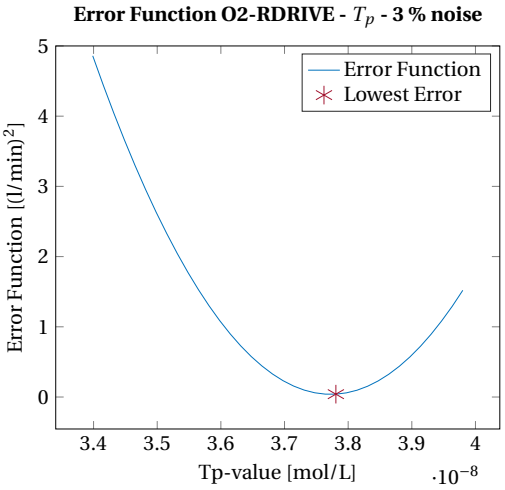

(c) *Error function. Estimation of T_p - 3% noise.*

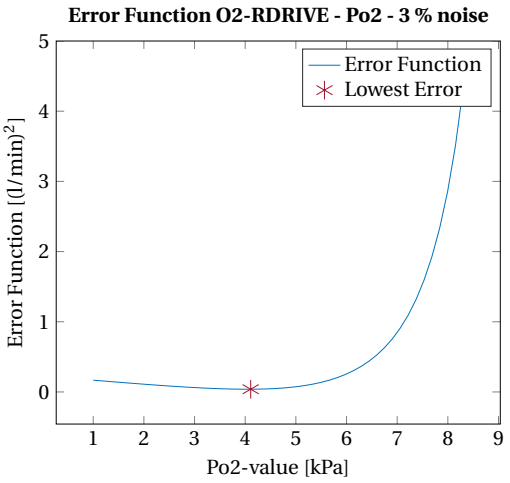

(d) *Error function. Estimation of Po2 - 3% noise.*

Figure 6.7: *Error functions between estimated and measured $\dot{V}A$ for T_p and Po2 respectively. Simulations both with and without noise.*

The error functions of the $Po2$-estimations are shown in the right side figures (Figure 6.7(b), Figure 6.7(d), Figure 6.8(b) and Figure 6.8(d)). By inspecting the best $Po2$ found in the simulation data with 5% noise, Figure 6.8(b) and Figure 6.8(d), the estimated $Po2$ is approximately 6 kPa which is 2 kPa from the original 4 kPa which is indicating, that the $Po2$-parameter for itself may not uniquely describe D_p for a patient.

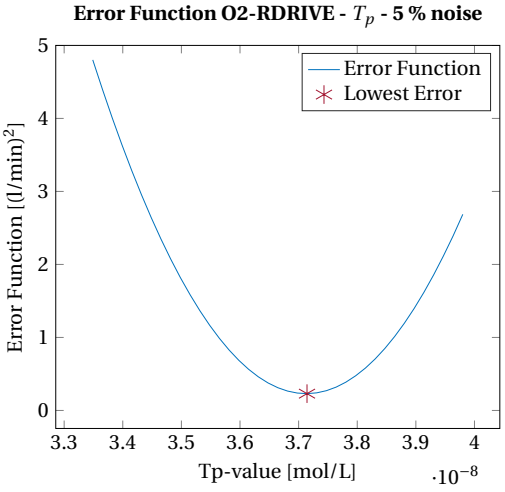

(a) *Error function. Estimation of Tp - 5 % noise.*

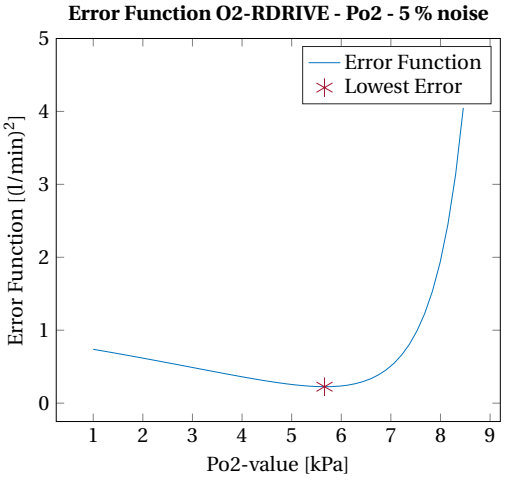

(b) *Error function. Estimation of Po2 - 5 % noise.*

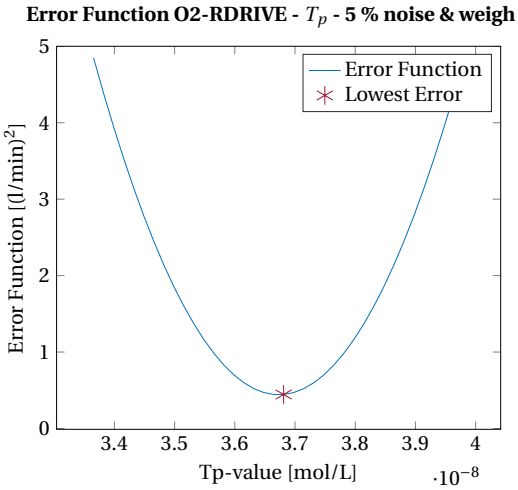

(c) *Error function. Estimation of Tp - 5 % noise - weigh 5.*

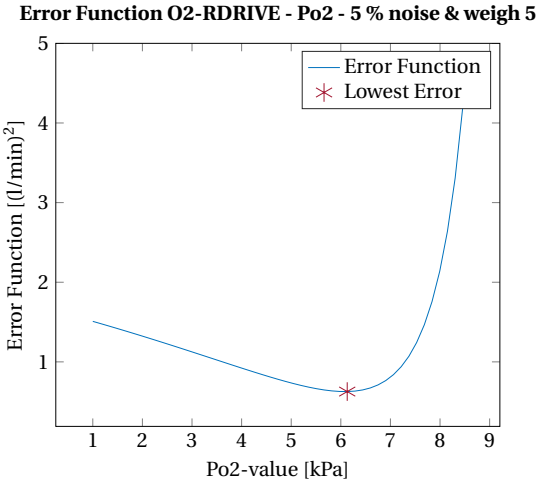

(d) *Error function. Estimation of Po2 - 5 % noise - weigh 5.*

Figure 6.8: *Error function between estimated and measured va for Tp and Po2 respectively. Simulations with noise both with and without weighing.*

The error functions for the two parameter grid search of T_p and $Po2$ can be seen in Figure 6.9. These four sub-figures show the 3-dimensional error functions using the color scale from yellow to blue, where dark blue indicate lowest error. The same trend of a low error (dark blue) going in a line across the plots from left to right are seen in all the figures. The area of equally low error indicates that the values of both T_p and $Po2$ can not be uniquely identified in the simulation data, hence the same results are expected in real patient data. On this basis the two parameter grid search method is not used.

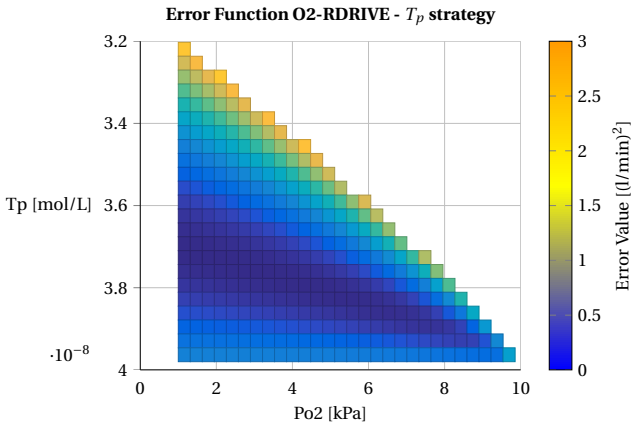

(a) *Error function. Estimation of Tp and Po2 - noise free.*

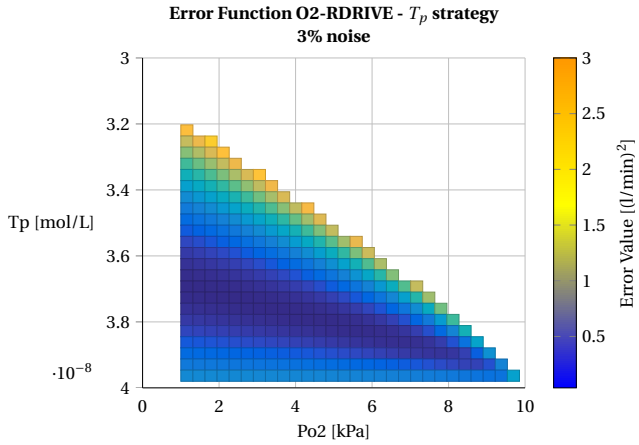

(b) *Error function. Estimation of Tp and Po2 - 3 % noise.*

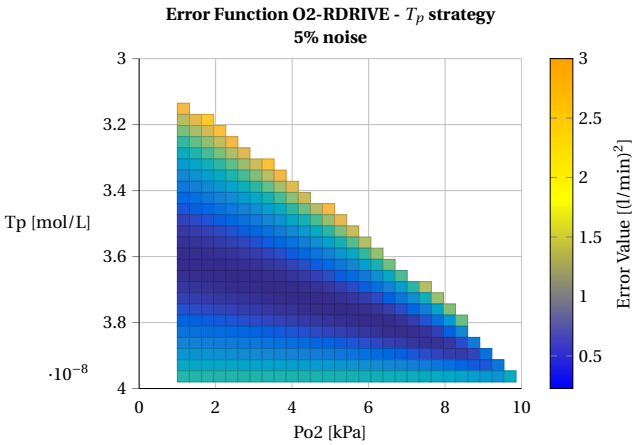

(c) *Error function. Estimation of Tp and Po2 - 5 % noise.*

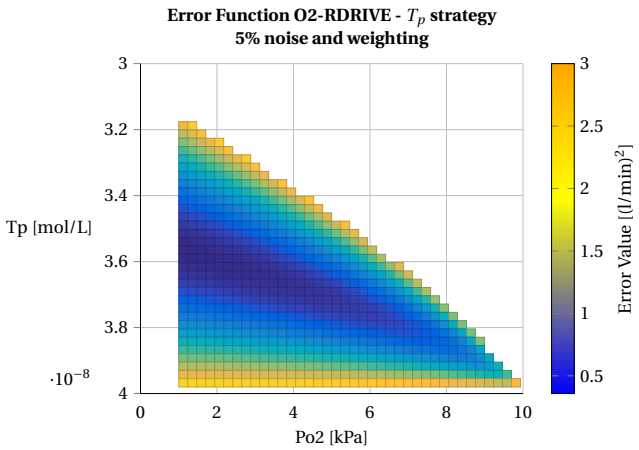

(d) *Error function. Estimation of Tp and Po2 - 5 % noise - weight 5.*

Figure 6.9: *2D visualization of the 3D Error functions between estimated and simulated $\dot{V}A$ for T_p and $Po2$. The more dark blue, the lower the error value. Simulations with noise both with and without weighing.*

In order to obtain the low MSE found by the two parameter grid search method and to combine this with unique identifiability for the parameters, the T_p-strategy was tested. This method first estimates T_p, where A and $Po2$ are constants, and then estimates $Po2$ to the estimated T_p-value. The error function is illustrated in Figure 6.10. The logic behind this method, is that the T_p-parameter can uniquely be identified alone as indicated by the red line in Figure 6.10(a). In Figure 6.10(a) T_p has a low error in the dark blue area. By using the patient-specific value of T_p, the $Po2$ value can now be estimated with a reasonable low error. T_p is chosen to be estimated first as this parameter is thought to provide best physiological meaning.

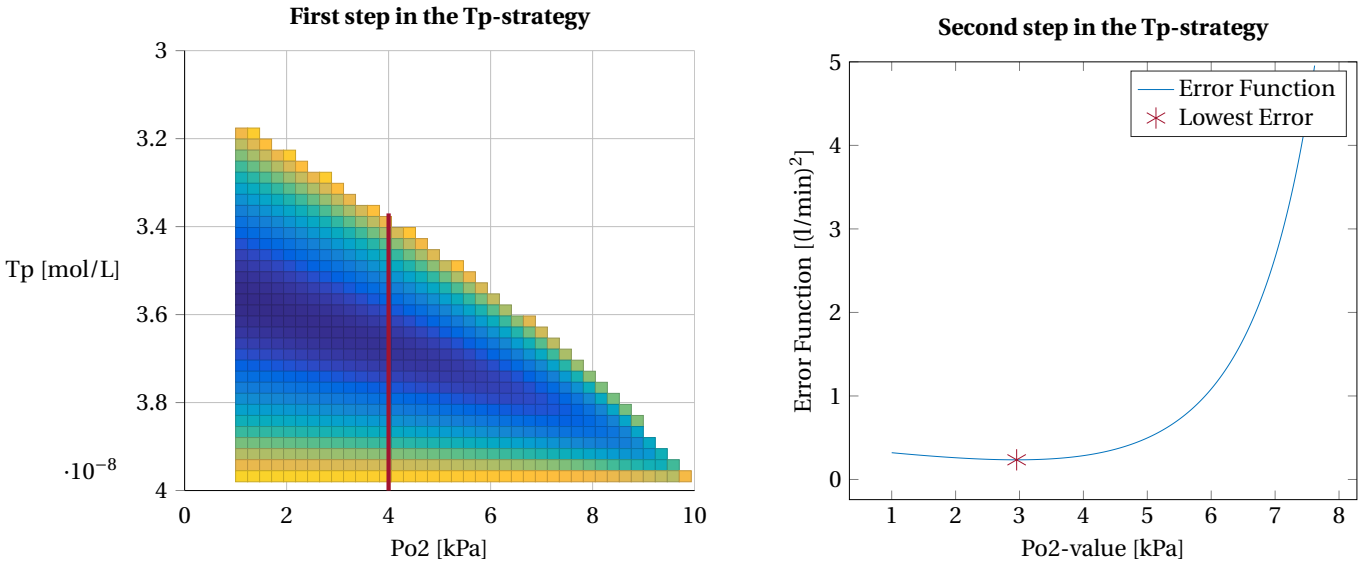

(a) *Estimation of Tp for simulated data with 5% noise. The high $F_{et}O_2$ are weighed with 5. The T_p value with lowest error is 36.73·10^{-9} mol/L.*

(b) *Estimation of Po2 using the estimated T_p value from Figure 6.10(a).*

Figure 6.10: *Error functions between estimated and simulated $\dot{V}A$ for Tp-strategy. T_p are estimated first as indicated with the red line in Figure 6.7(a). Po2 is estimated with the found T_p. No weighs are used in the error function in Figure 6.7(b)*

To validate, that the estimated values of T_p and $Po2$ using the T_p-strategy can uniquely be found for the simulated data, the estimated $Po2$ will be used to estimate the T_p value, hence using the method in backwards order. The validation will be performed on the simulation data with 5% added noise and weighs used in the error calculation. By using this backwards-validation method, T_p is estimated to 36.76 nmol/l with a difference of 0.03 nmol/l from the first estimation. On this basis the T_p-strategy is believed to uniquely estimate the parameters. As seen in Figure 6.10(b), the estimated $Po2$ is close to 3 kPa, which is an error of approximately 1 kPa from the original simulated ideal data $Po2$ value. By comparing this result with the best $Po2$ es-

timation using the $Po2$ method alone, see Figure 6.8(d), $Po2$ is closer to the original value (4 kPa) using the T_p-strategy.

6.4 Wakefulness Drive Estimation

The wakefulness drive is by Ainslie & Duffin described to be the drive to breathe, that is independent on chemoreflexes and absent during sleep. From Duffin, 2005 D_w is assumed to add 7 l/min to the minute volume equal to a $\dot{V}A$ at 5.2 l/min (assuming a normal respiratory frequency at 12 breaths/min and 150 ml dead space). The value of D_w is only added to the total drive to breath, when the two chemoreflexes are activated [Duffin, 2005]. Hereby it should be noted, that D_w is used by Larraza et al. as a constant ventilation contribution (2 l/min) to add up the chemoreflex ventilation.

The original value of a D_w contribution of 2 l/min from the RDRIVE model will at first be used in the parameter estimation in this thesis. However, by preliminary analysis of the peripheral drive estimation, the value of D_w can have a considerable effect on the estimated values of $\dot{V}A$. This can be the case, if the RDRIVE-estimated D_c plus D_w are larger than the measured $\dot{V}A$ at the high F_iO_2 (implying a negative D_p). The estimation of drive parameters is largely effected by the weigh used in the error function at the high F_iO_2 measurement resulting in non-accurate estimations of $\dot{V}A$.

To solve this problem, the value of D_w will be considered in each patient to ensure, that the combined value of D_w and D_c is lower than the measured $\dot{V}A$ at the highest F_iO_2 measurement. If they are higher, the residual between the two values will be subtracted from D_w. The pseudo code for this is listed in Listing 6.1. This procedure is found to provide better estimation results and assumed to being ascribed to the physiological description of the parameter.

Listing 6.1: *Pseudo code for the calculation of D_w*

```
if ((VAesti(High FiO2))>(VAmeas(High FiO2)))
    Dw = 2 - (VAesti(High FiO2)-VAmeas(High FiO2));
     else
    Dw = 2;
end
```

6.5 Measurement Data

The RDRIVE model will be tested on respiration measurements from 6 COPD patients. These patients are chosen from a cohort of COPD patients used in a previous study [Thomsen et al., 2012].

The experimental data is measured with the clinical tool ALPE, [Thomsen et al., 2013], which is described in Section 3.1. COPD patients

have a depressed central drive, why they are more dependent on their peripheral drive, see Section 2.3. The literature states that ventilation response should increase as response to decreased inspired oxygen fractions [Lumb, 2010]. The respiratory response function of inspired oxygen is expected to be an exponential decreasing function, as the peripheral drive sensitivity is from the literature assumed to increase in response to low arterial oxygen [Duffin, 2005; Larraza et al., 2014].

The test of the model will therefore be focused on patient data, which show increased ventilation to decreased inspired oxygen. By inspection of the available patient data, 6 patients show this response, why they will represent the experimental data, see Table 6.3.

Patient	Sex	Age	P_aCO_2	P_aO_2	BMI	COPD diagnose	fs	$fA2$	$f2$	BE
1	M	75	4.65	10.40	21	Severe	0.01	0.72	0.99	-0.64
2	M	76	6.54	8.89	29	Severe	0.10	0.83	0.99	4.49
3	M	81	4.40	11.40	24	Moderate	0.04	0.56	0.91	-2.60
4	M	53	5.70	8.40	27	Very severe	0.13	0.77	0.99	1.55
5	M	62	4.84	8.78	24	Very severe	0.13	0.55	0.64	-0.37
6	M	66	5.50	10.4	34	Moderate	0.04	0.66	0.97	2.12

Table 6.3: *Patient demographics*

As seen in the patient demographics, the patients are all diagnosed with moderate or worse COPD diagnosis. The gas exchange parameters (fs, $fA2$ and $f2$) indicate that some of the patients are having respiratory impairments (patient 4 and 5 showing 13% shunt for instance). However the blood parameter BE show that only two patients are outside the normal range of -2 to 2.

6.5.0.1 Measurement Errors

Measurement errors are always present [Cobelli & Carson, 2008]. There exist some known errors which are correlated with the measured ventilation data. Firstly, from a physiological point of view, the ventilation measurements were expected to be more consistent in response to low inspired oxygen fractions. This unexpected respiratory response is shown in Figure 6.11. From Figure 6.11 it can be seen that the $\dot{V}$A at 0.14 $F_{et}O_2$ is higher than the $\dot{V}$A measured at 0.12 $F_{et}O_2$. This situation is unexpected. This could be due to difficulties in relation to the measurements them-self, where the patients needed to breath through an oxygen mask, which applies more resistance than normal breathing.

The blood sample measurement was performed when the patients breathed atmospheric air. The arterial blood parameters are expected to change due to changed inspired oxygen, why the ventilation measurement at all other times can not be related to measured

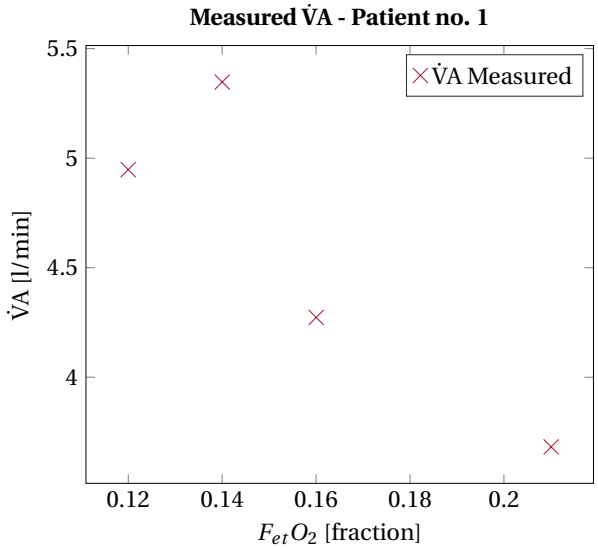

Figure 6.11: *Patient example of unexpected V̇A response to change in oxygen.*

blood values, e.g. blood oxygen pressure. Furthermore, the performed blood sample itself can have an effect on ventilation, because the patients experienced some stress related with fear and pain of the arterial puncture. This affect is believed to be seen in the first two ALPE-measurements.

The measurement equipment can likewise cause measurement errors. The measurement accuracy of the pulse oximeter is related with an error of ±2 %, which can affect the estimations of the ALPE-parameters, which are used throughout the RDRIVE-model. Gas and flow measurements are likewise believed to contribute with a small error contribution. From a theoretical point of view, it can be difficult to account for several errors simultaneously [Cobelli & Carson, 2008].

PART III

RESULTS

CHAPTER 7

Model Validation

The following section will represent the results of the four different methods of parameter estimation that was described in Section 6.2.

The results will be represented as plots of the estimated and measured $\dot{V}A$ for all patients in order to illustrate how the parameter estimation affects the estimation of $\dot{V}A$, compared to the estimated $\dot{V}A$ from the RDRIVE model, see Figure 7.1. For each patient the plot will contain:

- Measured $\dot{V}A$ for that patient
- Estimated $\dot{V}A$ using the RDRIVE model
- Estimated $\dot{V}A$ using the O2-RDRIVE model with estimated Tp
- Estimated $\dot{V}A$ using the O2-RDRIVE model with estimated $Po2$
- Estimated $\dot{V}A$ using the O2-RDRIVE T_p-strategy with estimated T_p and $Po2$

Besides the measured and estimated $\dot{V}A$, the error functions for estimation of T_p and $Po2$ are illustrated, see Figure 7.2 and Figure 7.3.

The results will be discussed in Chapter 8.

7.1 Evaluation of Estimated and Measured V̇A

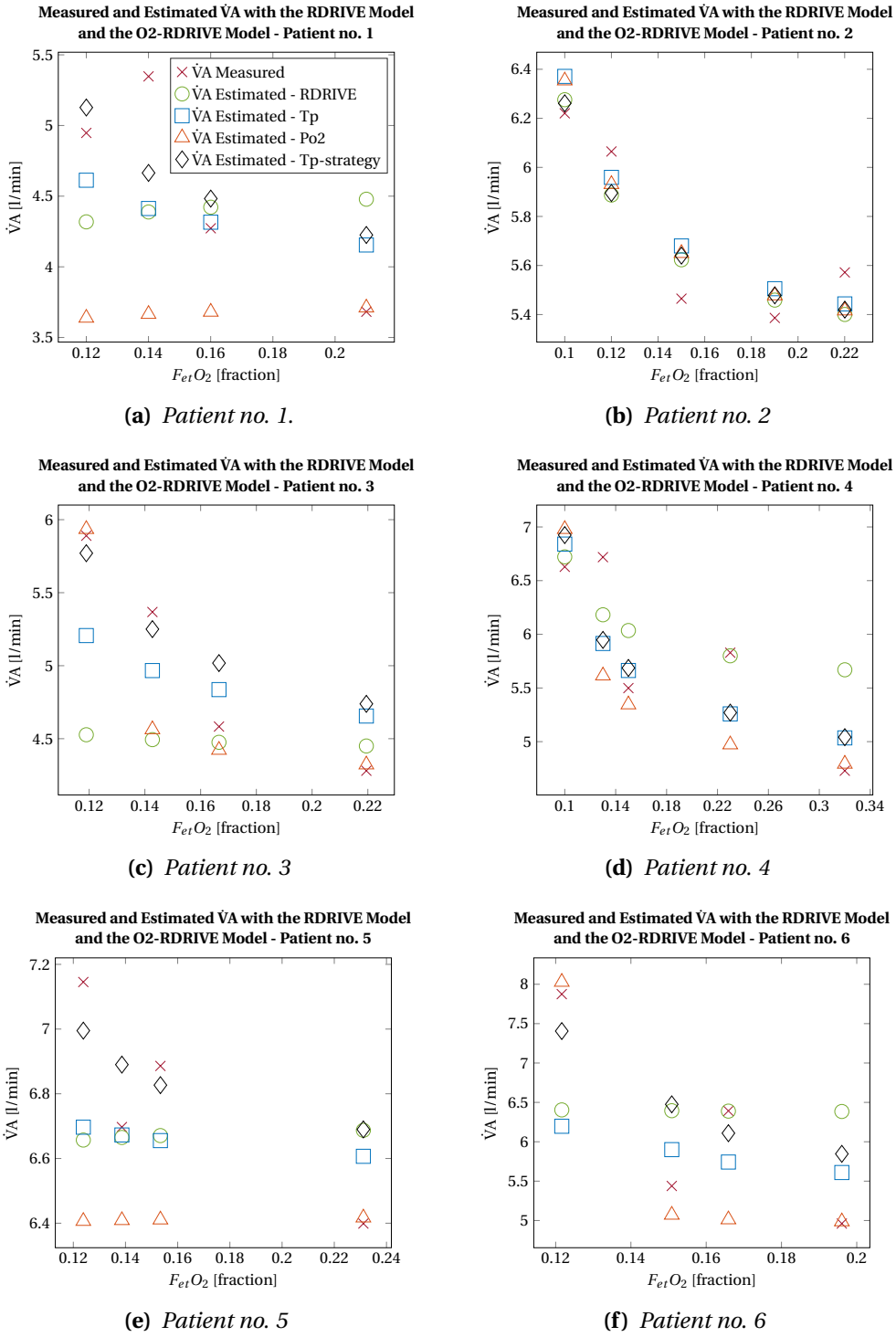

(a) *Patient no. 1.*

(b) *Patient no. 2*

(c) *Patient no. 3*

(d) *Patient no. 4*

(e) *Patient no. 5*

(f) *Patient no. 6*

Figure 7.1: *Estimated and measured V̇A for the 6 patients and all four parameter estimation methods. Each symbol represents an estimation method. Please see the symbol description in the plot for Patient no. 1*

7.2 Error Functions of Tp parameterization

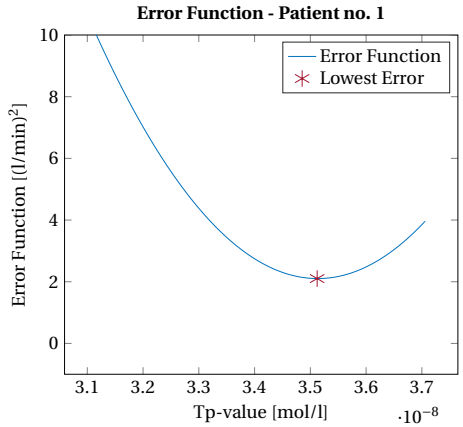

(a) *Patient no. 1.*

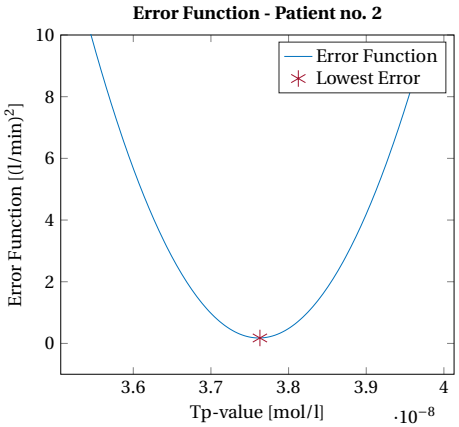

(b) *Patient no. 2*

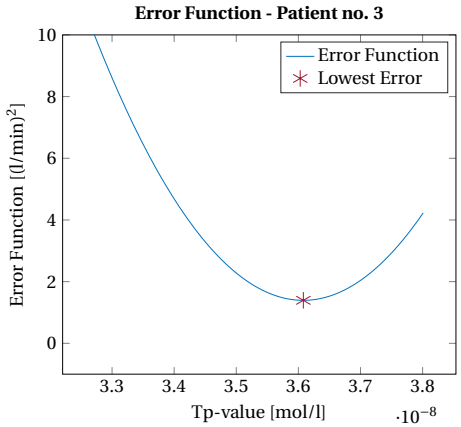

(c) *Patient no. 3*

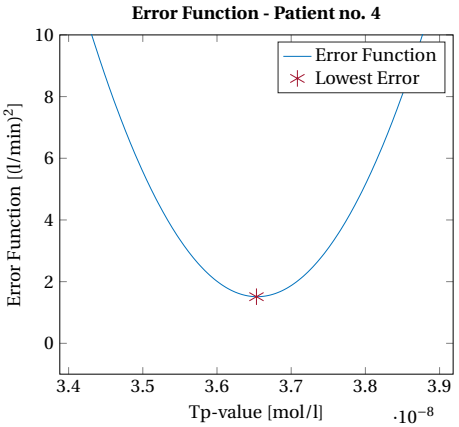

(d) *Patient no. 4*

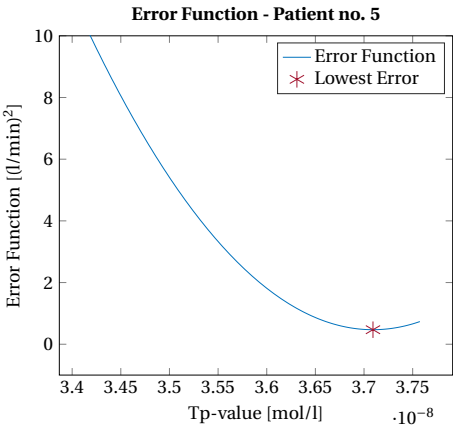

(e) *Patient no. 5*

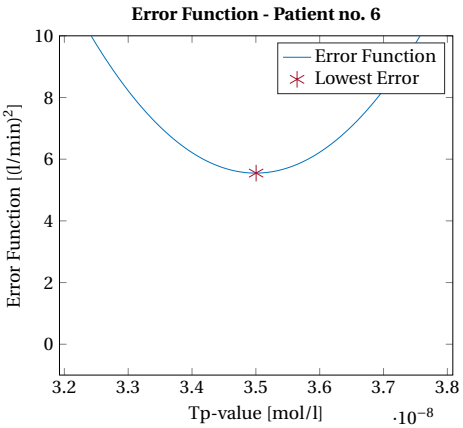

(f) *Patient no. 6*

Figure 7.2: *Error Function between measured and estimated $\dot{V}A$ when estimating Tp using the O2-RDRIVE model.*

7.3 Error Functions of Po2 parameterization

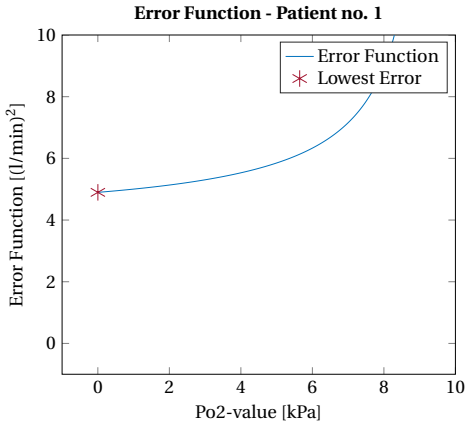

(a) *Patient no. 1.*

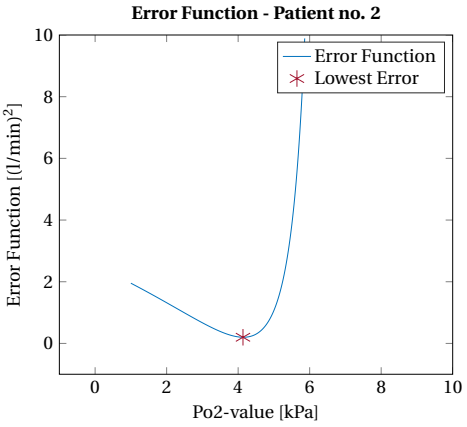

(b) *Patient no. 2*

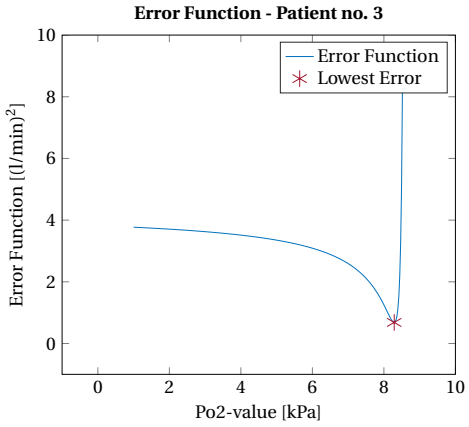

(c) *Patient no. 3*

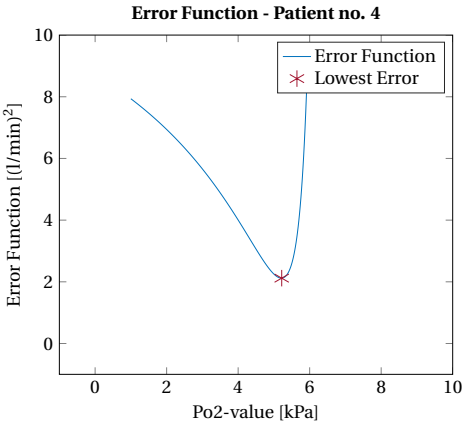

(d) *Patient no. 4*

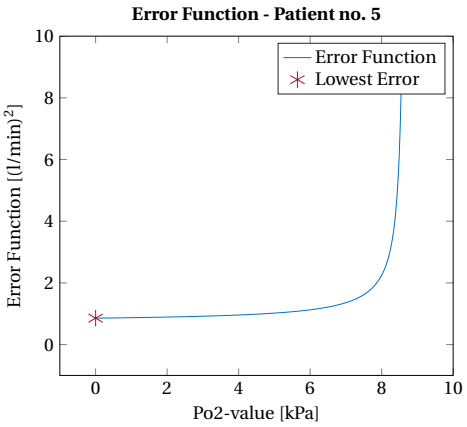

(e) *Patient no. 5*

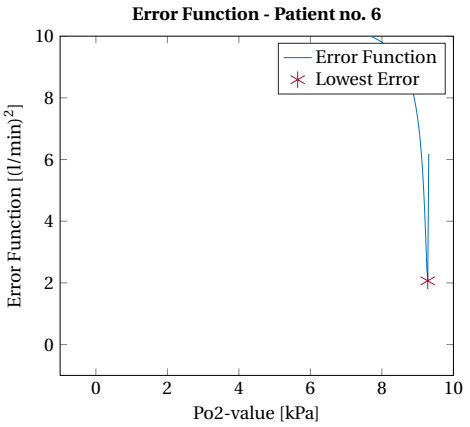

(f) *Patient no. 6*

Figure 7.3: *Error Function between measured and estimated $\dot{V}A$ when estimating Po2 using the O2-RDRIVE model.*

7.4 Result tables

The results are shown in tables for which the mean error between the estimated $\dot{V}A$ and the measured $\dot{V}A$ is represented for every patient. The mean error is used as not all patients have the same number of measurements of $\dot{V}A$. Besides the mean error the estimated patient parameter(s) for that particular method is represented.

Table 7.1 lists the mean squared error for each patient with the use of the RDRIVE model. Table 7.2 lists the mean squared error and the estimated T_p-value, when using the O2-RDRIVE model. Likewise Table 7.3 lists the mean squared error and estimated value of $Po2$, when using the O2-RDRIVE model. Table 7.4 lists the results when estimating T_p first and then $Po2$.

In Table 7.5 the summed mean squared error between measured and estimated $\dot{V}A$ is listed for all the tested methods.

Table 7.6 lists the means of the three peripheral drive parameters for all six patients. These three values are a mean of the values, found for the three parameters estimated using the T_p-strategy. The A value is constant for all patients.

Patient no.	Mean Squared Error $[(\mathrm{l/min})^2]$
1	0.493
2	0.019
3	0.665
4	0.294
5	0.092
6	1.275

Table 7.1: *Result of estimation with the RDRIVE model. Mean squared error between measured $\dot{V}A$ and estimated $\dot{V}A$. $A = 2.3733\ l \cdot kPa\ (min \cdot nM \cdot l^{-1})^{-1}$, $T_p = 37.748$ nmol/l and $Po2 = 4$ kPa.*

Patient no.	Mean Squared Error $[(\mathrm{l/min})^2]$	Estimated T_p [nmol/l]
1	0.303	35.122
2	0.022	37.631
3	0.366	36.08
4	0.228	36.532
5	0.075	37.092
6	0.967	35.004

Table 7.2: *Result of parameter estimation of T_p. Mean squared error between measured $\dot{V}A$ and estimated $\dot{V}A$. $A = 2.3733\ l \cdot kPa\ (min \cdot nM \cdot l^{-1})^{-1}$ and $Po2 = 4$ kPa.*

Patient no.	Mean Squared Error $[(\mathrm{l/min})^2]$	Estimated $Po2$ [kPa]
1	1.224	0.001
2	0.020	4.135
3	0.169	8.289
4	0.421	5.218
5	0,214	0.001
6	0.516	9.282

Table 7.3: *Result of parameter estimation of Po2. Mean squared error between measured $\dot{V}A$ and estimated $\dot{V}A$. T_p = 37.748 nmol and A = 2.3733 $l \cdot kPa\ (min \cdot nM \cdot l^{-1})^{-1}$.*

Patient no.	Mean Squared Error $[(\mathrm{l/min})^2]$	Estimated T_p value [nmol/l]	Estimated Po2 [kPa]
1	0.209	35.122	6.222
2	0.093	37.631	3.798
3	0.427	36.08	5.697
4	0.225	36.532	4.087
5	0.148	37.092	6.603
6	0.539	35	6.624

Table 7.4: *Result of parameter estimation with the T_p-strategy. Mean squared error between measured $\dot{V}A$ and estimated $\dot{V}A$. A = 2.3733 $l \cdot kPa\ (min \cdot nM \cdot l^{-1})^{-1}$.*

Tested method	RDRIVE	T_p-estimated	$Po2$-estimated	T_p-strategy
Mean error $[(l/min)^2]$	0.394	0.300	0.427	0.189

Table 7.5: *Summed mean squared error between measured and estimated $\dot{V}A$ for all patients for the four tested methods.*

Parameter	T_p (± SD) [nmol/l]	$Po2$ (± SD) [kPa]	A [l · kPa (min · nM · l^{-1})$^{-1}$]
Mean Patient	36.243 (0.962)	5.505 (1.15)	2.3733

Table 7.6: *Mean value of the three parameters used to describe the peripheral drive using the T_p-strategy.*

PART IV

SYNTHESIS

CHAPTER 8

Discussion

The discussion consists of three sections. The first section will discuss the results in this thesis, the next section will discuss the assumptions that were made in order to perform the parameterization of the peripheral respiratory drive and the last section will discuss the usefulness of the O2-RDRIVE model.

In the postoperative period where anesthesia and analgesia are still wearing off the respiratory drive might be impaired because of these drugs. Furthermore, patients diagnosed with COPD are known to have a decreased central respiratory response to CO_2 [Larraza et al., 2015b; Lumb, 2010]. If the peripheral drive in this patient group is also impaired, the patients could be less responsive to changes in oxygen as well as changes in CO_2. Hence it is assessed that parameterization of the respiratory drive can help clinicians in optimizing patient treatment thereby avoiding unwanted situations like postoperative hypoxemia. Recent studies have shown that a modeling approach can be used to parameterize the central drive from clinically available data [Larraza et al., 2015a,b, 2014].

Through this discussion, the aspects of whether and how a modeling approach may be used to estimate peripheral respiratory drive in patients with spontaneous breathing will be discussed.

8.1 Discussion of the Results

Using a novel method for parameterization of the peripheral drive in spontaneously breathing patient, $\dot{V}A$ have been estimated for six patients as seen Figure 7.1 in Chapter 7. The results are evaluated both by reviewing the mean squared error to assess if each of the four different methods are estimating the peripheral drive accurately, and by visual inspection of the results in Figure 7.1. As the mean squared error only describes an overall error between the measured and estimated values of $\dot{V}A$, the visual inspection of the results is just as important.

In Figure 7.1 it can be seen, that for Patient no. 2 and no. 4, all the methods seems to give a good estimation of $\dot{V}A$. For Patient no. 2, the RDRIVE model estimates $\dot{V}A$ with a low error of 0.019 $(\text{l/min})^2$. For this patient, arterial pressure of oxygen and arterial concentration of H^+ matches the RDRIVE model's threshold value of $Po2$ and T_p in such a way, that the estimation of $\dot{V}A$ is accurate. This is though not the coincident for the rest of the patients, why these standard

threshold values are found not to provide a reliable estimation of $\dot{V}A$. The accuracy of the RDRIVE model's description of peripheral drive is consistent if the patient specific blood hydrogen ion concentration coincide with the constant parameter of T_p, why the RDRIVE model will provide seemingly good estimations of $\dot{V}A$ in Patient no. 2.

What should be noted is, that in the estimation of $\dot{V}A$ at F_iO_2 = 21% ($F_eO_2 \approx$ 15-16%), the RDRIVE model does estimate within a relatively small margin of error for all patients. This could indicate, that even though the estimation of the central drive is done at the highest available F_iO_2 for the individual patient, the "starting point" for the estimation of the parameters for the O2-RDRIVE model is offset.

The offset is only corrected in the estimation method of Po2. In Figure 7.1 it can be seen that estimation of $Po2$ before estimation of $\dot{V}A$ gives an estimation of $\dot{V}A$ at high F_iO_2 that is close to the measured $\dot{V}A$. Furthermore the estimation of Po2 estimates $\dot{V}A$ at low F_iO_2 with a small error in all patients except Patient no. 1 and no. 5. For these two patients, it can be seen in Figure 7.3(a) and Figure 7.3(e) that the lowest error is located at $Po2 \approx 0$. Visual inspection of the error function indicates, that a lower error could be found, if the values of $Po2$ was allowed to adapt to values below zero.

The method of estimating T_p before estimation of $\dot{V}A$ does not correct for the aforementioned offset in starting point $\dot{V}A$. In Patient no. 2 and no. 4 it does estimate $\dot{V}A$ adequately, but for the rest of the patients, the sensitivity to oxygen is too low. This makes estimation of $\dot{V}A$ at high F_iO_2 inadequate.

As mentioned in Section 6.2 the grid search algorithm was designed to weigh the error between estimated and measured $\dot{V}A$ greater at highest F_iO_2 than at the other measurement points. It was tested how a larger weighing would alter the aforementioned offset. Increasing the weighing does (naturally) give a more accurate estimation of $\dot{V}A$ at the high F_iO_2 level, but the response to changes in F_iO_2 is then depressed. A higher weighing was on this basis discarded.

The T_p-strategy is the method that, for the six patients, best describes the change in $\dot{V}A$ when changing F_iO_2. The method is not most accurate for all patients, as it is seen in Figure 7.1, but one should keep in mind that the measured $\dot{V}A$ is polluted with noise and in some cases (like in Figure 7.1(a), Figure 7.1(e) and Figure 7.1(f)), the measured $\dot{V}A$-response is non-expected. The expected response to lower F_iO_2 in short periods of time is an increase in respiratory response [Asmussen & Nielsen, 1957].

Table 7.4 shows the results of estimating $\dot{V}A$ with the T_p-strategy. The values of T_p is believed to best describe the specific patient response to oxygen, because T_p can be related to arterial hydrogen ion concentrations and is the physically definition of peripheral chemoreflex threshold. By inspection of the results, patient no. 2, 4 and 5 have

the highest estimated T_p of the six patients, however there is small difference to the rest of the patients' estimated T_p. Table 7.6 lists the mean parameter values obtained from the T_p-strategy and thereby describes a "mean COPD patient" in terms of respiratory drive parameters. From Table 7.6 the values indicate, that this specific patient group needs a lower threshold for T_p (36.243 nmol/l for the patient group vs. 37.748 nmol/l from [Larraza et al., 2014]) and a higher threshold for $Po2$ (5.505 kPa for the patient group vs. 4 kPa from [Larraza et al., 2014]).
This indicates that more patient specific parameter values could give a more accurate estimation of the patients actual response to changes in inspired oxygen.

8.2 Discussion of the Assumptions

This sections aims to discus some of the assumptions made in the use of the RDRIVE model and further in the parameterization of the peripheral drive.

Throughout the estimation of $\dot{V}A$ the arterial blood gases are assumed to be constant. Only the value of arterial PO_2 is recalculated for all values of F_iO_2. This assumption is done on basis of previous use of all the models used in this thesis [Larraza et al., 2014; Rees & Andreasen, 2005] and will not be discussed further.

The wakefullness is in this thesis used as a factor that corrects for the difference between measured and estimated $\dot{V}A$ at the highest F_iO_2. This assumption was done, as there to the best of our knowledge does not exist a clear definition of the wakefullness drive. Duffin uses a minute ventilation value of 7 l/min for D_w whereas Larraza et al. uses a $\dot{V}A$ value of 2 l/min for D_w. The latter is used because it *"in combination with disfacilitation for -1 $l \cdot min^{-1}$ from both central and peripheral drives allows the simulation of apnea"* - cited from [Larraza et al., 2014]. Because of the unknown definition of D_w and the different applications by Larraza et al. and Duffin, we decided to use the value as a factor for correction. The value of D_w is thereby allowed to change and describes the "extra $\dot{V}A$" from D_c to the estimated $\dot{V}A$.

8.3 Usefulness of O2-RDRIVE

The investigated methods to estimate peripheral drive parameters provide in general a more accurate description of $\dot{V}A$ in the included COPD patient group compared with using the RDRIVE model. Estimation of peripheral chemoreflex threshold (T_p) followed by an estimation of oxygen sensitivity ($Po2$) is found to be the best method to describe peripheral drive in regards to both lowest MSE and unique identifiability. This could be useful in both the patient group described in this thesis, but also in patients in general as knowledge

about the individual patient's respiratory response could help clinicians to provide better respiratory treatment to the patient.

A clinical example of the usefulness of the O2-RDRIVE model could be when treating COPD patients with mechanical ventilator support. The COPD patient group needs special attention because of the associated risk of hypo-ventilation caused by the dependence of their peripheral drive. The D_w parameters T_p and $Po2$ might be quantified to be used in decision support to find a maximum tolerated increase in inspired oxygen.

Patent for the RDRIVE model has been applied and the model is assumed to be a part of the already existing clinical bedside tool BEACON, that can be used for optimization of respiratory treatment.

The "mean COPD patient" represented in Table 7.6 illustrates that the parameters found in this patient group do not coincide with the patient group described by Larraza et al., 2015a,b, as only one patient in the COPD patient group can get the ventilation response adequately described by the RDRIVE model alone. This indicates that specific parameterization of the peripheral drive parameters gives a better description of the respiratory response in a patient group with impaired central drive.

8.4 Conclusion

In this thesis a novel method for individual patient parameterization of peripheral drive has been proposed and evaluated in a COPD patient group. The method may be used to describe and predict patients response to changes in oxygen treatment at the bedside.

Bibliography

Ainslie, P. N., & Duffin, J. (2009). Integration of cerebrovascular CO2 reactivity and chemoreflex control of breathing: mechanisms of regulation, measurement, and interpretation. *American Journal of Physiology-Regulatory, Integrative and Comparative Physiology*, *296*(5), R1473—-R1495.

Asmussen, E., & Nielsen, M. (1957). Ventilatory response to CO2 during work at normal and at low oxygen tensions. *Acta physiologica Scandinavica*, *39*(1), 27–35.

Bailey, P. L. (1996, December). Respiratory effects of postoperative opioid analgesia. *Seminars in Anesthesia, Perioperative Medicine and Pain*, *15*(4), 343–352. Retrieved from http://www.sciencedirect.com/science/article/pii/S027703269680047X

Cobelli, C., & Carson, E. (2008). *Introduction to modeling in physiology and medicine*. Academic Press.

Dahan, a., & Teppema, L. J. (2003). Influence of anaesthesia and analgesia on the control of breathing. *British Journal of Anaesthesia*, *91*(1), 40–49. doi: 10.1093/bja/aeg150

Duffin, J. (2005). Role of acid-base balance in the chemoreflex control of breathing. *Journal of applied physiology (Bethesda, Md. : 1985)*, *99*, 2255–2265. doi: 10.1152/japplphysiol.00640.2005

Francisco, N. a. (2007). Control of breathing: how to better understand the respiratory effects of opioids. *European Journal of Pain Supplements*, *1*(1), 61–65. doi: 10.1016/S1754-3207(08)60015-2

Hall, J. E. (2010). *Guyton and Hall Textbook of Medical Physiology*. Retrieved from https://www.google.dk/books?hl=da&lr=&id=Po0zyO0BFzwC&pgis=1

Hedenstierna, G. (2012, July). Oxygen and anesthesia: what lung do we deliver to the post-operative ward? *Acta anaesthesiologica Scandinavica*, *56*(6), 675–85. Retrieved from http://www.ncbi.nlm.nih.gov/pubmed/22471648

Karbing, D. S., Kjærgaard, S., Andreassen, S., Espersen, K., & Rees, S. E. (2011). Minimal model quantification of pulmonary gas exchange in intensive care patients. *Medical engineering & physics*, *33*(2), 240–248. Retrieved from http://dx.doi.org/10.1016/j.medengphy.2010.10.007 doi: 10.1016/j.medengphy.2010.10.007

Karbing, D. S., Kjærgaard, S., Smith, B. W., Espersen, K., Allerœd, C., Andreassen, S., & Rees, S. E. (2007). Variation in the PaO2/FiO2 ratio with FiO2: mathematical and experimental description, and clinical relevance. *Critical care (London, England)*, *11*(6), R118. doi: 10.1186/cc6174

Kjærgaard, S., Rees, S., Malczynski, J., Nielsen, J. A., Thorgaard, P., Toft, E., & Andreassen, S. (2003). Non-invasive estimation of shunt and ventilation-perfusion mismatch. *Intensive care medicine*, *29*(5), 727–734.

Larraza, S., Dey, N., Karbing, D. S., Jensen, J. B., Nygaard, M., Winding, R., & Rees, S. E. (2015a). A mathematical model approach quantifying patients ' response to changes in mechanical ventilation : Evaluation in pressure support.

Larraza, S., Dey, N., Karbing, D. S., Jensen, J. B., Nygaard, M., Winding, R., & Rees, S. E. (2015b). A mathematical model approach quantifying patients ' response to changes in mechanical ventilation : Evaluation in volume support. *Medical Engineering and Physics*, *000*, 1–9. Retrieved from `http://dx.doi.org/10.1016/j.medengphy.2014.12.006` doi: 10.1016/j.medengphy.2014.12.006

Larraza, S., Dey, N., Karbing, D. S., Nygaard, M., Winding, R., & Rees, S. E. (2014). A mathematical model for simulating respiratory control during support ventilation modes. , 8433–8438.

Lumb, A. (2010). *Nunn's applied respiratory physiology* (7th ed.). Elsevier Health Sciences.

Rees, S. E. (2011). The Intelligent Ventilator (INVENT) project: The role of mathematical models in translating physiological knowledge into clinical practice. *Computer methods and programs in biomedicine*, *104*, S1—-S29.

Rees, S. E., & Andreasen, S. (2005). Mathematical Models of Oxygen and Carbon Dioxide Storage and Transport: The Acid–Base Chemistry of Blood. *Critical Reviews in Biomedical Engineering*, *33*(3), 209–264.

Rees, S. E., Kjærgaard, S., Thorgaard, P., Malczynski, J., Toft, E., & Andreassen, S. (2002). The Automatic Lung Parameter Estimator (ALPE) system: Non-invasive estimation of pulmonary gas exchange parameters in 10-15 minutes. *Journal of clinical monitoring and computing*, *17*(1), 43–52.

Rees, S. E., Klæstrup, E., Handy, J., Andreassen, S., & Kristensen, S. R. (2010). Mathematical modelling of the acid-base chemistry and oxygenation of blood: A mass balance, mass action approach including plasma and red blood cells. *European Journal of Applied Physiology*, *108*(3), 483–494. doi: 10.1007/s00421-009-1244-x

Rosenberg, J., Oturai, P., Erichsen, C. J., Pedersen, M. H., & Kehlet, H. (1994). Effect of general anesthesia and major versus minor surgery on late postoperative episodic and constant hypoxemia. *Journal of clinical anesthesia*, *6*(3), 212–216.

Siggaard-Andersen, O. (1974). *The acid-base status of the blood* (4th ed.). Munksgaard.

Siggaard-Andersen, O., Wimberley, P. D., Fogh-Andersen, N., & Gœthgen, I. H. (1988). Measured and derived quantities with modern pH and blood gas equipment: Calculation algorithms with 54 equations. *Scandinavian Journal of Clinical and Laboratory Investigation*, *48*, 7–15. doi: 10.3109/00365518809168181

Stewart, P. A. (1983). Modern quantitative acid-base chemistry. *Canadian journal of physiology and pharmacology*, *61*(12), 1444–1461.

Thomsen, L. P., Karbing, D. S., Smith, B. W., Murley, D., Weinreich, U. M., Kjærgaard, S., … Rees, S. E. (2013). Clinical refinement of the automatic lung parameter estimator (ALPE). *Journal of clinical monitoring and computing*, *27*(3), 341–350.

Thomsen, L. P., Weinreich, U. M., Karbing, D. S., & Rees, S. E. (2012). Measuring gas exchange with step changes in inspired oxygen: An analysis of the assumption of oxygen steady state. *IFAC Proceedings Volumes (IFAC-PapersOnline)*, *28*(6), 507–511. doi: 10.3182/20120829-3-HU-2029.00048

Thomsen, L. P., Weinreich, U. M., Karbing, D. S., & Rees, S. E. (2014). Measuring gas exchange with step changes in inspired oxygen: An analysis of the assumption of oxygen steady stateThomsen, L. P., Weinreich, U. M., Karbing, D. S., & Rees, S. E. (2014). Measuring gas exchange with step changes in inspired oxygen: An analys. *Journal of Clinical Monitoring and Computing*, *28*(6), 547–558. doi: 10.3182/20120829-3-HU-2029.00048